



ALL INFORMATION CONTAINED HEREIN IS UNCLASSIFIED  
DATE 08-14-2010 BY 60322 UCBAW/SJS

Technical Report HL-93-4  
May 1993

2

# A Three-Dimensional Numerical Model Study for the Chesapeake and Delaware Canal and Adjacent Bays

by **Bernard E. Hsieh, Billy H. Johnson,  
David R. Richards**  
*Hydraulics Laboratory*

**SD** DTIC  
ELECTE  
JUL 01 1993  
**AD**

Approved For Public Release; Distribution Is Unlimited

**93-14873**



93 6 30 0 27

Prepared for U.S. Army Engineer District, Philadelphia

The contents of this report are not to be used for advertising, publication, or promotional purposes. Citation of trade names does not constitute an official endorsement or approval of the use of such commercial products.



PRINTED ON RECYCLED PAPER

Technical Report HL-93-4  
May 1993

# A Three-Dimensional Numerical Model Study for the Chesapeake and Delaware Canal and Adjacent Bays

by Bernard B. Hsieh, Billy H. Johnson,  
David R. Richards

Hydraulics Laboratory

U.S. Army Corps of Engineers  
Waterways Experiment Station  
3909 Halls Ferry Road  
Vicksburg, MS 39180-6199

DTIC QUALITY INSPECTED 8

Approved For	
NTIS ORIGIN	<input checked="" type="checkbox"/>
DTIC ORIGIN	<input type="checkbox"/>
DTIC ORIGIN	<input type="checkbox"/>
By	
DTIC ORIGIN	
Availability Codes	
Dist	Approved For Special
A-1	

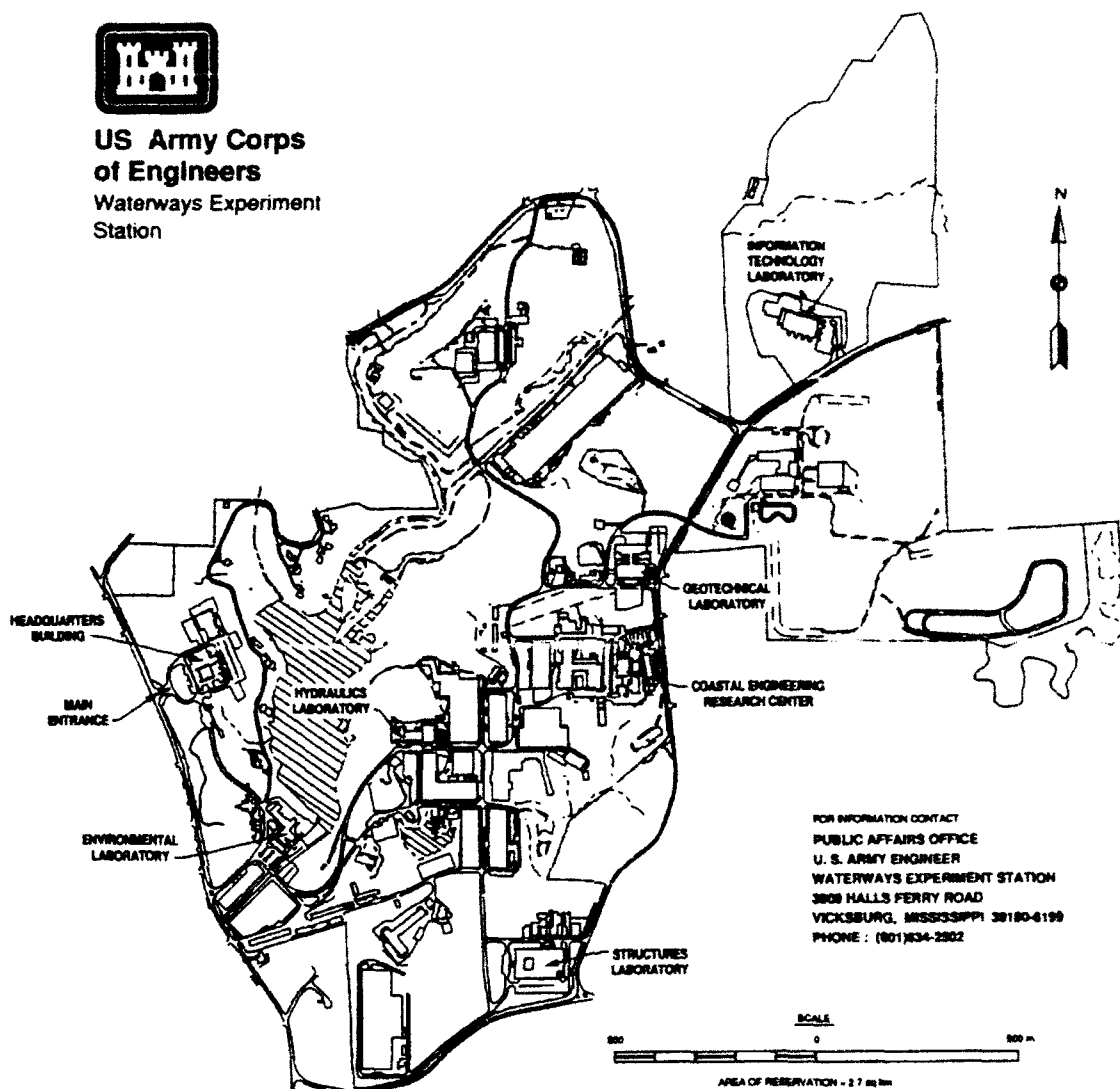
Final report

Approved for public release; distribution is unlimited

Prepared for U.S. Army Engineer District, Philadelphia  
Philadelphia, PA 19106-2991



**US Army Corps  
of Engineers**  
Waterways Experiment  
Station



**Waterways Experiment Station Cataloging-in-Publication Data**

Hsieh, Bernard Bor-Nian.

A three-dimensional numerical model study for the Chesapeake and Delaware Canal and adjacent bays / by Bernard B. Hsieh, Billy H. Johnson, David R. Richards ; prepared for U.S. Army Engineer District, Philadelphia.

55 p. : ill. ; 28 cm. — (Technical report ; HL-93-4)

Includes bibliographical references.

1. Chesapeake and Delaware Canal (Del. and Md.) — Mathematical models. 2. Intra-coastal waterways — Maryland — Mathematical models. 3. Canals — Delaware — Mathematical models. 4. Harbors — Hydrodynamics — Mathematical models. I. Johnson, Billy H. II. Richards, David R., P. Eng. III. United States. Army. Corps of Engineers. Philadelphia District. IV. U.S. Army Engineer Waterways Experiment Station. V. Title. VI. Series: Technical report (U.S. Army Engineer Waterways Experiment Station) ; HL-93-4. TA7 W34 no.HL-93-4

# Contents

---

Preface .....	iv
Conversion Factors, Non-SI to SI (Metric) Units of Measurement .....	v
1—Introduction .....	1
Physical Description .....	1
Overview of Previous Work .....	4
Scope of Work .....	4
2—Theoretical Basis of C&D Canal 3-D Hydrodynamic Model .....	6
Basic Equations .....	6
Nondimensionalization of Equations .....	8
External-Internal Modes .....	9
Boundary-Fitted Equations .....	11
Boundary Conditions .....	12
Initial Conditions .....	13
Solution Algorithm .....	13
Turbulence Parameterization .....	14
Numerical Grid .....	15
3—The C&D Canal 3-D Hydrodynamic Model .....	17
Grid Generation .....	17
Database Development .....	17
Forcing Functions .....	18
Verification of the Homogeneous Model .....	25
Final Month-Long Verification .....	27
3-D Tidally Averaged Circulation .....	30
4—Net Transport Due to Channel Deepening .....	39
5—Conclusions and Recommendations .....	45
Conclusions .....	45
Recommendations .....	45
References .....	47
SF 298	

# Preface

---

In February of 1989, the Hydraulics Laboratory (HL) of the U.S. Army Engineer Waterways Experiment Station (WES), Vicksburg, MS, was requested by the U.S. Army Engineer District, Philadelphia (CENAP), to conduct an investigation of possible tidal flow and salt changes in the Chesapeake and Delaware Canal area caused by the proposed deepening plans using a three-dimensional numerical hydrodynamic model. Results from the study were intended to provide long-term simulation of hypothetical boundary variations for addressing many management issues and related environmental impacts and water resources management problems.

The study was funded by CENAP and conducted by HL personnel under the general direction of Messrs. F. A. Herrmann, Jr., Director, HL; R. A. Sager, Assistant Director, HL; W. H. McAnally, Chief, Estuaries Division (ED), HL; D. R. Richards, Chief, Estuarine Simulation Branch, ED; and J. B. Letter, former Chief of Estuarine Simulation Branch. Principal investigators and authors of this report were Dr. B. B. Hsieh, Estuarine Simulation Branch, Dr. B. H. Johnson, HL; and Mr. Richards.

At the time of publication of this report, Director of WES was Dr. Robert W. Whalin. Commander was COL Leonard G. Hassell, EN.

# Conversion Factors, Non-SI to SI (Metric) Units of Measurement

---

Non-SI units of measurement used in this report can be converted to SI  
(metric) units as follows:

Multiply	By	To Obtain
cubic feet	0.02831685	cubic meters
feet	0.3048	meters

# 1 Introduction

---

## Physical Description

The Chesapeake and Delaware (C&D) Canal is a sea-level, man-made canal which joins two large estuarine systems (Figures 1a and 1b). This canal was originally designed for barges and was later expanded to accommodate moderate size ships transiting between Chesapeake and Delaware Bays. The canal from Reedy Point on the Delaware Estuary to Welch Point on the Elk River, a tributary of the Upper Chesapeake Bay, is about 28 kilometers long. The most recent enlargement of the canal to accommodate larger vessels was started in 1963 and completed in late 1975. The resulting cross-section has an authorized depth of 35 ft (10.7 m) below mean low water and a bottom width of 450 ft (137.2 m). By comparison, the cross section before the enlargement was 27 ft (8.2 m) by 250 ft (76.2 m). A 1987 hydrographic survey indicated the average depth of the canal is about 40 ft (12.2 m). The dredged channel was constructed with a side slope of 2:1.

Due to the more complicated geometry and the longer travel distance from the Chesapeake Bay side, the C&D canal receives stronger tidal signals from the Delaware Bay mouth. Najarian (1980) indicated that tidal flow in the canal is controlled by the Delaware Estuary at its eastern boundary with a mean tide range of 5.5 ft (1.68 m) and by the Chesapeake Bay at its western boundary with a mean tide range of 2.2 ft (0.67 m). There is a phase lag of 10 hr on the average between the tides on the eastern and western boundaries. This causes large tidal fluxes, often over 88,200 cfs (2500 cms) (Rives and Pritchard, 1978) and maximum tidal currents of 1.07 mps (3.5 fps). The net flow through the canal changes from easterly to westerly in accordance with tidal amplitudes, phases, and densities at the two canal boundaries. In addition, this area experiences an average freshwater discharge of 1266 cms (44,700 cfs) from the Susquehanna River in Upper Chesapeake Bay. Nontidal contributions to the circulation in the Chesapeake and Delaware system also include wind-driven currents and gravitational flows due to gradients of density formed by freshwater runoff and seawater. The resultant flow in this system is also influenced by the Coriolis effect and frictional drag due to bottom roughness (Hires, 1983).



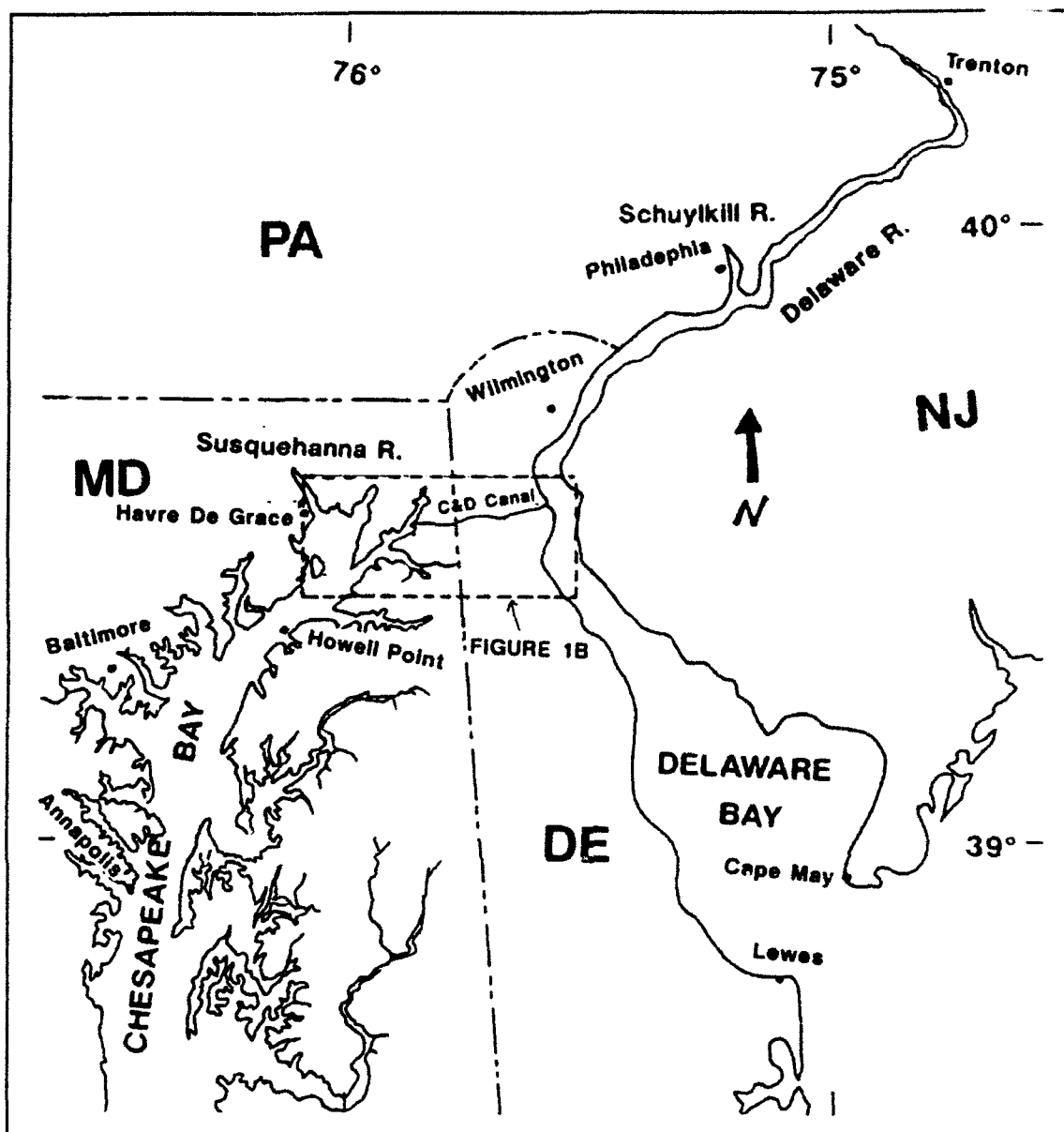


Figure 1a. C&D Canal and adjacent estuaries

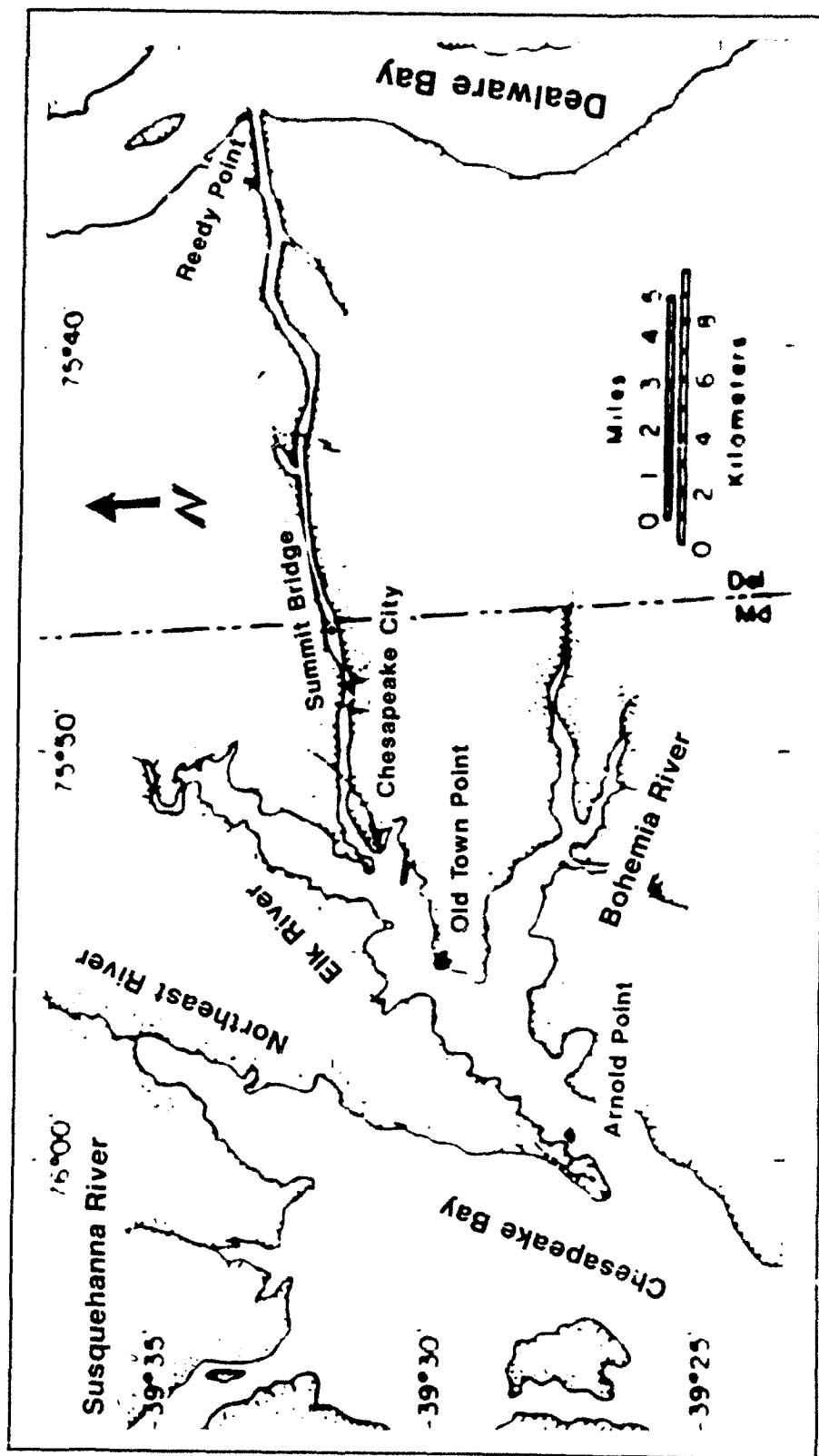


Figure 1b. C&D Canal System

## Overview of Previous Work

The C&D Canal flow problem has received much attention over the years. Historically, many investigations have been made in an attempt to describe the complex flows and salinity variations that have resulted from changing the C&D canal from its original locked system to its existing free-flowing form. However, due to the complex interactions of forcing functions and the sensitivity of flow conditions in the canal to hydraulic head differences, previous investigators have been unable to completely resolve questions related to the long-term transport of flow and salt through the canal.

The first known attempt at estimating mean flow in the C&D canal was made by C. F. Wicker (1938) from USACE, Philadelphia District. He found that during his 10 tidal cycle observations, there was a nontidal eastward flow of about 1,000 cfs. Boyd et al. (1973) studied the canal with a physical model and a one-dimensional (1-D) mathematical model and showed a nontidal eastward flow of about 2,000 cfs. Johnson (1974) developed a 1-D numerical model to address flow control for the C&D canal. Pritchard and Gardner (1974) revised the earlier estimate of mean eastward flow through the canal (988 cfs before enlargement; 2450 cfs after enlargement). They also reported a statistical analysis of long-term current and tidal elevation observations between 1969 and 1972. A net easterly nontidal flow from the Chesapeake to the Delaware occurred 59% of the time. Rives and Pritchard (1978) used data in April and May of 1975 to verify a one-dimensional model and concluded a westerly nontidal flow of 1,400 cfs. Several other investigators have reported that the C&D canal has a significant impact on the salt concentration and on the overall circulation of Delaware Bay.

Two Waterways Experiment Station (WES) three-dimensional (3-D) numerical study efforts have been accomplished that are related to the C&D canal area. A jointly funded effort by the US Army Corps of Engineers and the Environmental Protection Agency to develop a time-varying 3-D model of the complete Chesapeake Bay and its major tributaries resulted in the development of the computer code CH3D-WES that has been employed in the present study. Details are provided by Johnson et. al. (1989), Kim, Johnson and Sheng (1989), and Johnson et. al. (1991). This same code was employed in the development of a relatively fine grid 3-D model of the Upper Chesapeake Bay for the State of Maryland (Johnson, Heath and Kim (1989)). In both of the studies noted above, the C&D Canal was considered to be closed. A 3-D study performed by Galperin and Mellor (1990) to explore the tidal flow and salinity transport of the Delaware Bay-Continental Shelf system also treated the C&D Canal as closed.

## Scope of Work

With the modern supercomputer's development, three-dimensional, time-dependent, numerical modeling of complex estuarine systems has become a rapidly maturing field of research. To better understand the effect of one

estuarine system on the other and to accurately compute flow and mass fluxes through the canal, a 3-D numerical hydrodynamic model extending from the Chesapeake Bay Bridge at Annapolis, MD, through the C&D canal and connecting with a grid extending from Trenton, NJ, to the mouth of Delaware Bay has been developed. The 3-D model can be used to provide insight into the net transport through the canal for various forcing conditions over different averaging periods as well as to study the impact of enlarging the canal beyond its current size.

As noted, the particular computer code used is called CH3D-WES (Curvilinear Hydrodynamics in Three Dimensions). The basic code was developed by Sheng (1986) for WES but was extensively modified during the Chesapeake Bay study discussed previously. As its name implies, CH3D-WES makes hydrodynamic computations on a curvilinear or boundary-fitted planform grid. Physical processes impacting baywide circulation and vertical mixing that are modeled include tides, wind, density effects (salinity and temperature), freshwater inflows, turbulence, and the effect of the earth's rotation. The numerical grid employed in the 3-D hydrodynamic model was generated by the code WESCORR developed by Thompson and Johnson (1985). There were 873 active horizontal cells and a maximum of 12 vertical layers, resulting in 3325 computational cells. To capture the important bathymetric features and resulting hydrodynamics of the system, the vertical grid spacing was set at 1.52 m for the entire grid while horizontal spacing varied from about 800 m in the upper Chesapeake to 9000 m in the lower Delaware Bay. Basic input required for operation of the model are the time-varying water surface elevation and salinity distribution at the Annapolis and Cape May boundaries, an initial salinity field, wind data from Baltimore-Washington International Airport and Wilmington, and freshwater inflows from the Susquehanna, Delaware and Schuylkill Rivers. Basic output for comparison with observed data are water surface elevations at Havre De Grace, Reedy Point, Philadelphia, Old Town Point, and Chesapeake City, tidal currents at the Summit Bridge and Arnold Point, and the salinity distribution at the Summit Bridge, Arnold Point, Howell Point, and Reedy Point.

A limited review of the theoretical basis of CH3D-WES is described in Part II. More details are given by Johnson et. al. (1991) and Sheng (1986). The detailed discussion of the development of the C&D Canal 3-D model and subsequent verification are described in Part III. A month-long simulation was conducted for the purpose of comparing circulation patterns and net transport with field data. A discussion of net transport computations through the canal for 35, 40 and 45 ft channel depth alternatives is presented in Part IV. Part V summarizes the modeling results and offers technical recommendations.

## 2 Theoretical Basis of C&D Canal 3-D Hydrodynamic Model

---

As previously noted, the basic CH3D model was developed by Sheng (1986), but substantial changes have been made by WES. These changes have consisted of different basic formulations as well as extensive recoding for more efficient computing. Much of the presentation of material below has been taken from Sheng (1986) and the reader should refer to that reference as well as Johnson et. al. (1991) for more details.

### Basic Equations

The basic equations for an incompressible fluid in a right-handed Cartesian coordinate system  $(x,y,z)$  are:

$$\frac{\partial u}{\partial x} + \frac{\partial v}{\partial y} + \frac{\partial w}{\partial z} = 0 \quad (1)$$

$$\begin{aligned} \frac{\partial u}{\partial t} + \frac{\partial u^2}{\partial x} + \frac{\partial uv}{\partial y} + \frac{\partial uw}{\partial z} = & f_v - \frac{1}{\rho_o} \frac{\partial p}{\partial x} + \frac{\partial}{\partial x} \left( A_H \frac{\partial u}{\partial x} \right) \\ & + \frac{\partial}{\partial y} \left( \frac{A_H}{\partial y} \frac{\partial u}{\partial y} \right) + \frac{\partial}{\partial z} \left( A_v \frac{\partial u}{\partial z} \right) \end{aligned} \quad (2)$$

$$\frac{\partial v}{\partial t} + \frac{\partial uv}{\partial x} + \frac{\partial v^2}{\partial y} + \frac{\partial vw}{\partial z} = -f_u - \frac{1}{\rho_o} \frac{\partial p}{\partial y} + \frac{\partial}{\partial x} \left( A_H \frac{\partial v}{\partial x} \right)$$

$$+ \frac{\partial}{\partial y} \left( A_H \frac{\partial u}{\partial y} \right) + \frac{\partial}{\partial z} \left( A_v \frac{\partial u}{\partial z} \right) \quad (3)$$

$$\frac{\partial p}{\partial z} = - \rho g \quad (4)$$

$$\begin{aligned} \frac{\partial T}{\partial t} + \frac{\partial u T}{\partial x} + \frac{\partial v T}{\partial y} + \frac{\partial w T}{\partial z} \\ = \frac{\partial}{\partial x} \left( K_H \frac{\partial T}{\partial x} \right) + \frac{\partial}{\partial y} \left( K_H \frac{\partial T}{\partial y} \right) + \frac{\partial}{\partial z} \left( K_v \frac{\partial T}{\partial z} \right) \end{aligned} \quad (5)$$

$$\begin{aligned} \frac{\partial S}{\partial t} + \frac{\partial u S}{\partial x} + \frac{\partial v S}{\partial y} + \frac{\partial w S}{\partial z} \\ = \frac{\partial}{\partial x} \left( K_H \frac{\partial S}{\partial x} \right) + \frac{\partial}{\partial y} \left( K_H \frac{\partial S}{\partial y} \right) + \frac{\partial}{\partial z} \left( K_v \frac{\partial S}{\partial z} \right) \end{aligned} \quad (6)$$

$$\rho = \rho (T, S) \quad (7)$$

where  $(u, v, w)$  are velocities in  $(x, y, z)$  directions,  $f$  is the Coriolis parameter defined as  $2\Omega \sin\phi$  where  $\Omega$  is the rotational speed of the earth and  $\phi$  is the latitude,  $\rho$  is density,  $p$  is pressure,  $T$  is temperature,  $S$  is salinity,  $(A_H, K_H)$  are horizontal turbulent eddy coefficients, and  $(A_v, K_v)$  are vertical turbulent eddy coefficients. Equation 4 implies that vertical accelerations are negligible and thus the pressure is hydrostatic.

Various forms of the equation of state can be used for Eq. (7). In the present model, the following equation is used:

$$\rho = P/(\alpha + 0.698P)$$

where

$$P = 5890 + 38T - 0.375 T^2 + 3S$$

$$\alpha = 1779.5 + 11.25T - 0.0745T^2 - (3.8 + 0.10T) S, \quad (8)$$

with  $T$  in degrees C,  $S$  in ppt, and  $\rho$  in  $\text{gm/cm}^3$ .

## Nondimensionalization of Equations

Working with the dimensionless form of the governing equations makes it easier to compare the relative magnitude of various terms in the equations. With the subscript "r" referring to arbitrary reference values, the following dimensionless variables are used:

$$(u^*, v^*, w^*) = (u, v, wX_r/Z_r) / U_r$$

$$(x^*, y^*, z^*) = (x, y, zX_r/Z_r) / X_r$$

$$(\tau_x^*, \tau_y^*) = (\tau_x, \tau_y) / \rho_o f Z_r U_r$$

$$t^* = tf$$

$$\zeta^* = g\zeta / f U_r X_r = \zeta / S_r$$

$$\rho^* = (\rho - \rho_o) / (\rho_r - \rho_o) \quad (9)$$

$$T^* = (T - T_o) / (T_r - T_o)$$

$$A_H^* = A_H / A_{Hr}$$

$$A_v^* = A_v / A_{vr}$$

$$K_H^* = K_H / K_{Hr}$$

$$K_v^* = K_v / K_{vr}$$

which then yields the following dimensionless parameters in the governing equations:

$$\text{Vertical Ekman Number:} \quad E_v = A_{vr}/fZ_r^2$$

$$\text{Lateral Ekman Number:} \quad E_H = A_{Hr}/fX_r^2$$

$$\text{Vertical Prandtl (Schmidt) Number:} \quad Pr_v = A_{vr}/K_{vr}$$

$$\text{Lateral Prandtl (Schmidt) Number:} \quad Pr_H = A_{Hr}/K_{Hr}$$

$$\text{Froude Number:} \quad Fr = U_r/(gZ_r)^{1/2} \quad (10)$$

$$\text{Rossby Number:} \quad Ro = U_r/fX_r$$

$$\text{Densimetric Froude Number:} \quad Fr_D = Fr / \sqrt{\epsilon}$$

$$\text{where} \quad \epsilon = (\rho_r - \rho_o)/\rho_o$$

The dimensionless Cartesian equations can be found in Sheng (1986).

## External-Internal Modes

The basic Equations (1-4) can be integrated over the depth to yield a set of vertically integrated equations for the water surface,  $\zeta$ , and unit flow rates  $U$  and  $V$  in the  $x$  and  $y$  directions. Using the dimensionless variables (asterisks have been dropped) and parameters previously defined, the vertically integrated equations constituting the external mode are:

$$\frac{\partial \zeta}{\partial t} + \beta \left( \frac{\partial U}{\partial x} + \frac{\partial V}{\partial y} \right) = 0 \quad (11)$$

$$\frac{\partial U}{\partial t} = -H \frac{\partial \zeta}{\partial x} + \tau_{sx} - \tau_{bx} + V$$



$$\begin{aligned}
& - Ro \left[ \frac{\partial}{\partial x} \left( \frac{UU}{H} \right) + \frac{\partial}{\partial y} \left( \frac{UV}{H} \right) \right] \\
& + E_H \left[ \frac{\partial}{\partial x} \left( A_H \frac{\partial U}{\partial x} \right) + \frac{\partial}{\partial y} \left( A_H \frac{\partial U}{\partial y} \right) \right] \\
& - \frac{Ro}{Fr_D^2} \frac{H^2}{2} \frac{\partial p}{\partial x}
\end{aligned} \tag{12}$$

$$\begin{aligned}
\frac{\partial V}{\partial t} = & - H \frac{\partial \zeta}{\partial y} + \tau_{sy} - \tau_{by} - U \\
& - Ro \left[ \frac{\partial}{\partial x} \left( \frac{UV}{H} \right) + \frac{\partial}{\partial y} \left( \frac{VV}{H} \right) \right] \\
& + E_H \left[ \frac{\partial}{\partial x} \left( A_H \frac{\partial V}{\partial x} \right) + \frac{\partial}{\partial y} \left( A_H \frac{\partial V}{\partial y} \right) \right] \\
& - \frac{Ro}{Fr_D^2} \frac{H^2}{2} \frac{\partial p}{\partial y}
\end{aligned} \tag{13}$$

$$\text{where } \beta = gZr/f^2 X_r^2 = (R_o/F_r)^2$$

As will be discussed later, the major purpose of the external mode is to provide the updated water surface field.

Similarly, using the previously defined dimensionless parameters the internal mode equations become:

$$\begin{aligned}
\frac{\partial hu}{\partial t} = & - h \frac{\partial \zeta}{\partial x} + E_v \frac{\partial}{\partial z} \left( A_v \frac{\partial hu}{\partial z} \right) + hv \\
& - R_o \left( \frac{\partial hu u}{\partial x} + \frac{\partial huv}{\partial y} + \frac{\partial huw}{\partial z} \right)
\end{aligned}$$

$$\begin{aligned}
& + E_H \left[ \frac{\partial}{\partial x} \left( A_H \frac{\partial hu}{\partial x} \right) + \frac{\partial}{\partial y} \left( A_H \frac{\partial hu}{\partial y} \right) \right] \\
& - \frac{R_o}{Fr_D^2} \left( \int_z \frac{\partial \rho}{\partial x} dz \right)
\end{aligned} \tag{14}$$

$$\begin{aligned}
\frac{\partial hv}{\partial t} &= -h \frac{\partial \zeta}{\partial y} + E_v \frac{\partial}{\partial z} \left( A_v \frac{\partial hv}{\partial z} \right) - hu \\
& - R_o \left( \frac{\partial hvu}{\partial x} + \frac{\partial hvv}{\partial y} + \frac{\partial hvw}{\partial z} \right) \\
& + E_H \left[ \frac{\partial}{\partial x} \left( A_H \frac{\partial hv}{\partial x} \right) + \frac{\partial}{\partial y} \left( A_H \frac{\partial hv}{\partial y} \right) \right] \\
& - \frac{R_o}{Fr_D^2} \left( \int_z \frac{\partial \rho}{\partial y} dz \right)
\end{aligned} \tag{15}$$

$$\begin{aligned}
\frac{\partial hS}{\partial t} &= \frac{E_v}{Pr_v} \frac{\partial}{\partial z} \left( K_v \frac{\partial S}{\partial z} \right) - R_o \left( \frac{\partial huS}{\partial x} + \frac{\partial hvS}{\partial y} + \frac{\partial hwS}{\partial z} \right) \\
& + \frac{E_H}{Pr_H} \left[ \frac{\partial}{\partial x} \left( K_H \frac{\partial hS}{\partial x} \right) + \frac{\partial}{\partial y} \left( K_H \frac{\partial hS}{\partial y} \right) \right]
\end{aligned} \tag{16}$$

where  $(u, v, w)$  are the three components of the velocity and  $h$  is the layer thickness. If temperature,  $T$ , is being modelled, an additional equation that is identical to the transport-diffusion equation for salt is solved but using  $T$  instead of  $S$ . These three equations plus the internal continuity equation (Equation 1) constitute the internal mode of the C&D Canal and adjacent Bays Model.

## Boundary-Fitted Equations

To better resolve complex geometries in the horizontal directions, the C&D Canal model utilizes a boundary-fitted or generalized curvilinear grid. However, all computations are made on a transformed rectangular grid which necessitates the transformation of the governing equations presented above into

the boundary-fitted coordinates. The resulting equations are rather long and complex; therefore, the reader is referred to Sheng (1986) and Johnson et. al. (1991) for details of the transformation and a listing of the equations. It should be noted that both the  $x, y$  coordinates and the velocity are transformed. Therefore, contravariant components of the velocity rather than the physical components are computed. However, this is transparent to the user since the contravariant components are transformed back to the physical plane before being output. Again, the interested reader should refer to the above references. In addition to transforming the governing equations, a numerical boundary-fitted grid must be specified.

## Boundary Conditions

The boundary conditions at the free surface are:

$$A_v \left( \frac{\partial \bar{u}}{\partial z}, \frac{\partial \bar{v}}{\partial z} \right) = \frac{1}{\rho} (\tau_{sx}, \tau_{sy})$$

$$\frac{\partial T}{\partial z} = \frac{Pr}{E_v} K (T - T_e)$$

$$\frac{\partial S}{\partial z} = 0$$

whereas, the boundary conditions at the bottom are:

$$A_v \left( \frac{\partial \bar{u}}{\partial z}, \frac{\partial \bar{v}}{\partial z} \right) = \frac{1}{\rho} (\tau_{bx}, \tau_{by})$$

$$= \frac{U_r}{Av_r} Z_r C_d \left( \bar{u}_1^2 + \bar{v}_1^2 \right)^{1/2} (\bar{u}_1, \bar{v}_1)$$

$$\frac{\partial T}{\partial z}, \frac{\partial S}{\partial z} = 0$$

where  $K$  is the surface heat exchange coefficient,  $T_e$  is the equilibrium temperature,  $\bar{u}, \bar{v}$  are the contravariant horizontal components of the velocity,  $C_d$  is the bottom friction coefficient, and  $\bar{u}_1, \bar{v}_1$  are the values of the horizontal velocity components next to the bottom.  $C_d$  is determined from the Monin-Obukhov similarity relationships. Therefore, if  $z_1$  (one-half the bottom layer thickness) is within the constant flux layer,  $C_d$  is given by

$$C_d = k^2 \left[ \ln \left( z_1/z_o \right) \right]^{-2}$$

where  $k$  is the von Karman constant and  $z_o$  is the bottom roughness height.

Along the shoreline where river inflow occurs, the freshwater inflow and its temperature (if temperature is modeled) are prescribed and the salinity is assumed to be zero. At an ocean boundary, the water-surface elevation is prescribed along with time-varying vertical distributions of salinity and perhaps temperature. During flood, the specified values of salinity and temperature are employed; whereas, during ebb an advective condition is employed.

Along a solid boundary, both the normal velocity component and the viscosity are zero. In addition, the normal derivatives of temperature and salinity are zero.

## Initial Conditions

When initiating a run of the model, the values of  $\zeta$ ,  $\bar{u}$ ,  $\bar{v}$  and  $w$  are normally set to zero. Values of the salinity (and perhaps temperature) are read from an input file generated from known data at a limited number of locations.

## Solution Algorithm

Finite differences are used to replace derivatives in the governing equations, resulting in a system of linear algebraic equations to be solved.

### External Mode

The external mode consists of the surface displacement and the vertically integrated unit flows. With the finite-difference scheme employed, all of the terms in the continuity equation are treated implicitly; whereas, only the water surface slope terms in the momentum equations are treated implicitly. Those terms treated implicitly are weighted between the new and old time-steps. The resulting finite difference equations are then factored such that an x-sweep followed by a y-sweep of the horizontal grid yields the solution at the new time-step.

### Internal Mode

The internal mode of the Model consists of computations for the three velocity components and salinity. The only terms treated implicitly are the vertical diffusion terms in all equations and the bottom friction and surface slope terms in the momentum equations. Values of the water surface

elevations from the external model are used to evaluate the surface slope terms. As a result, the extremely restrictive speed of a free surface gravity wave is removed from the stability criteria.

It should be noted that once the  $\bar{u}$   $\bar{v}$  velocity components are computed, they are adjusted to ensure the conservative of mass. This is accomplished by forcing the sum of  $\bar{u}$  over the vertical to be the vertically averaged velocity  $\bar{U}/H$  and the sum of  $\bar{v}$  over the vertical to equal  $\bar{V}/H$ .  $\bar{U}$  and  $\bar{V}$  are the contravariant components of the vertically averaged unit flow rates.

## Turbulence Parameterization

Horizontal eddy viscosity and eddy diffusion coefficients are generally of relatively small importance in large scale environmental hydrodynamic models. Thus, these coefficients are treated as constants in the C&D Canal model. However, in order to adequately simulate 3-D estuarine flow fields a more sophisticated treatment of the vertical coefficients is required. A simplified turbulence model is employed.

The basic assumption in the derivation of the vertical turbulence closure model is that the turbulence is in a state of local equilibrium, i.e., turbulence generated at a point is dissipated at that point. Sheng (1982, 1984) shows that the vertical coefficients can be written as

$$A_v = S_m \Omega q$$

$$K_v = S_p \Omega q$$

where

$$q = f(Ri) \Omega \left| \frac{\partial \bar{v}}{\partial z} \right|$$

and both  $S_m$  and  $S_p$  are functions of the Richardson number  $Ri$ . In these equations,  $\Omega$  is the macro-scale of turbulence and must be prescribed to close the system. In addition to setting  $\Omega = 0.65z$  near the boundaries, three basic constraints are used to compute  $\Omega$  at the vertical position  $z$ . These constraints are

$$\left| \frac{d\Omega}{dz} \right| \leq 0.65$$

$$\Omega \leq \frac{q}{\left(-\frac{g}{\rho} \frac{\partial \rho}{\partial z}\right)^{0.5}}$$

$$\Omega \leq Q_{cut} \left( z_q = q_{max} - z_q = \frac{q_{max}}{2} \right)$$

where  $Q_{cut}$  is on the order of 0.15 to 0.25. The interested reader should refer to Sheng (1982, 1984, 1986) for a detailed discussion of the vertical turbulence parameterization.

## Numerical Grid

A staggered grid is used in both the horizontal and vertical directions of the computational domain (Figure 2). In the horizontal directions, a unit cell consists of a  $\zeta$ -point in the center ( $\zeta_{i,j}$ ), a  $U$ -point to its left ( $U_{i,j}$ ) and a  $V$ -point to its bottom ( $V_{i,j}$ ). In the vertical direction, the vertical velocities are

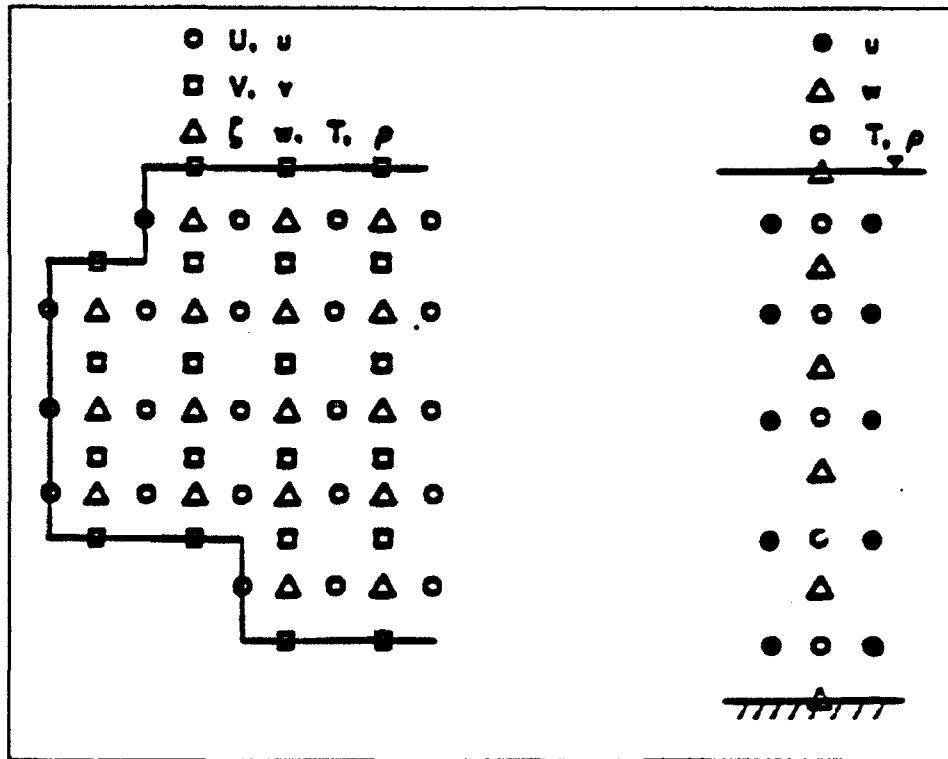
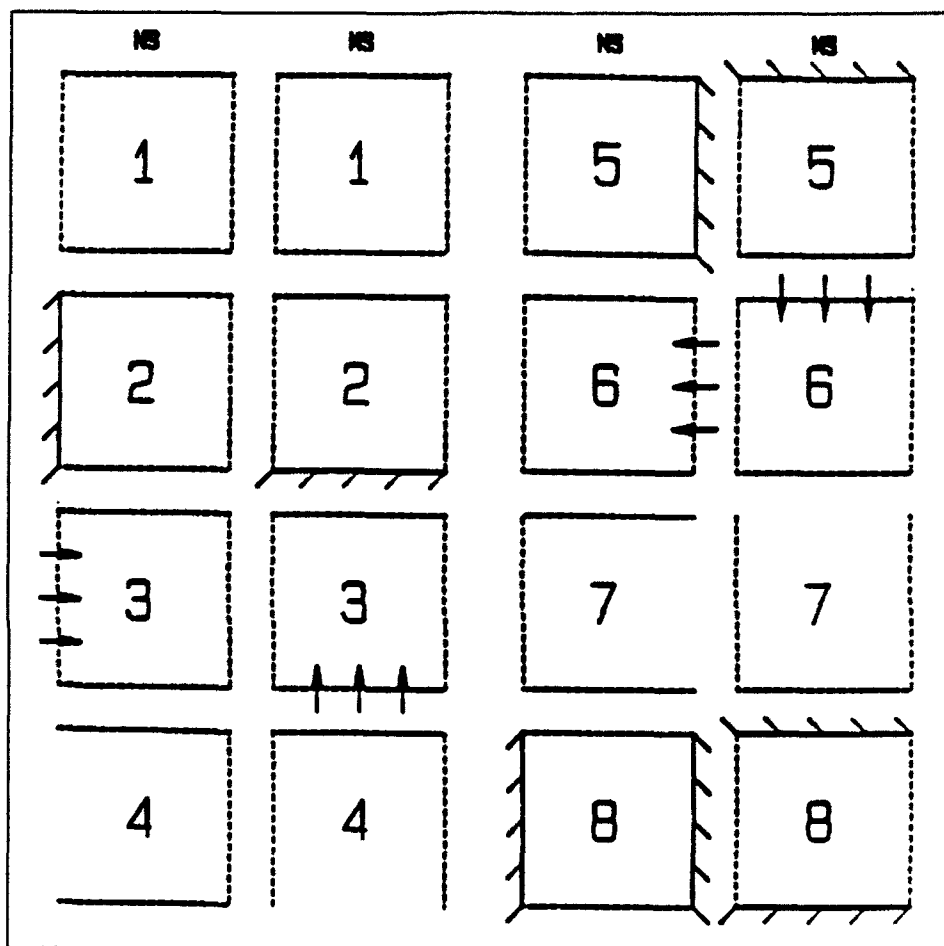


Figure 2. Staggered numerical grid

Two arrays, each of dimension (IMAX, JMAX), are used to index the grid cells. The array NS indicates the condition of the left and right cell boundaries, while the array MS denotes the condition of the top and bottom cell boundaries (Figure 3).



16

### **3 The C&D Canal 3-D Hydrodynamic Model**

---

A fully 3-D, time-dependent, numerical model of the C&D Canal and adjacent estuaries has been developed. In this study, particular care was given to the incorporation of the ocean forcing functions, surface wind stress, and freshwater runoff. Minor modifications of the CH3D computer code were required to handle this particular application with computational efficiency.

#### **Grid Generation**

A medium resolution 3-D numerical model grid of Upper Chesapeake Bay, a coarse 3-D grid of Delaware Bay, and a fine grid of the C&D Canal and its boundary area was developed with the grid generation software WESCORA (Figure 4). The Upper Chesapeake Bay grid is essentially the same grid employed by Johnson, Heath, and Kim (1989). This grid system has 81 cells in the x-direction, 50 cells in the y-direction, and 12 layers in the vertical, with all except the top layer being 1.52 m (5 ft) thick, though many of these cells are not computational cells. A total of 27 cells, each 3500 ft long by 450 ft wide, describes the canal. The main channel of the Delaware Bay, C&D Canal, and the navigable parts of the Upper Chesapeake Bay are represented as a 40-foot-deep waterway in the base condition. The minimum number of vertical layers at any point in the grid is two.

#### **Database Development**

To test and verify the 3-D model, a large database of prototype data are required. Several sources, including NOAA, EPA, and the State of Maryland, were contacted to determine the availability of field data. The State of Maryland conducted two eight-month surveys in 1985 over the C&D Canal, however, due to problems with the instruments, these could not be converted to a useful form, (personal communication with University of Maryland). During much of 1984, NOAA conducted a fairly extensive field data collection program on a portion of the system being modeled. Considering storm events, wind fluctuations, and the seasonality of freshwater inflow observed in the data, data from September of 1984 were selected to test and verify the model.



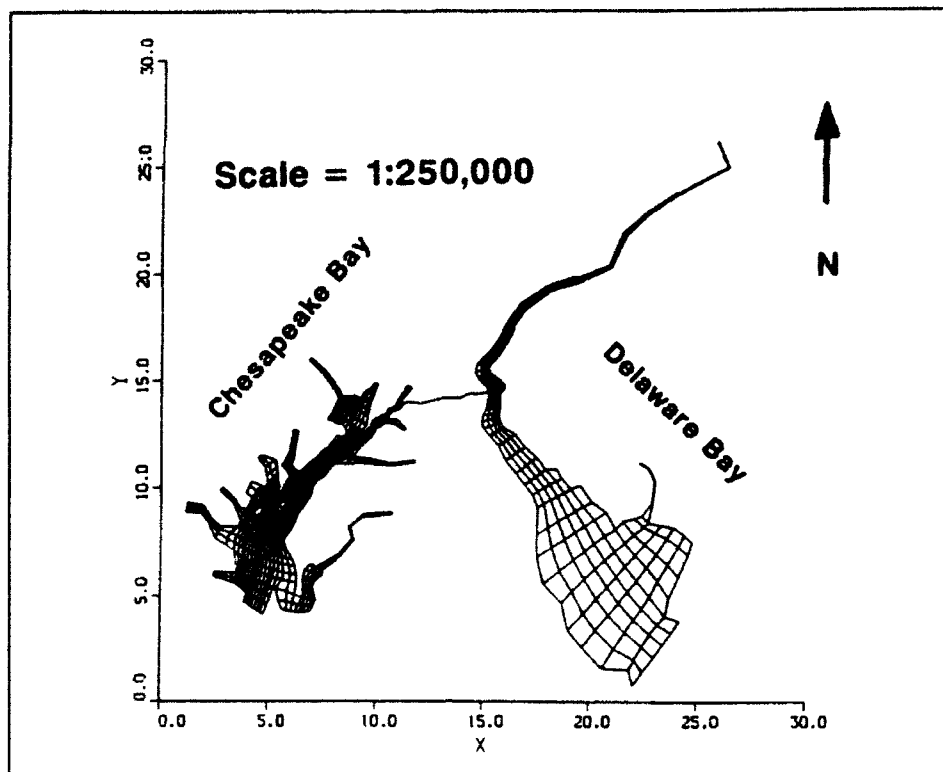


Figure 4. Computation grid

Tidal current and salinity data were collected at gauges near Summit Bridge, Arnold Point, Howell Point, and Reedy Point (salinity only) (Fig 1a-1b). However, an error in the current meter at Howell Point resulted in no information being produced during this period at that location. Water surface elevation data were collected at Annapolis, Havre De Grace, Cape May, Lewes, Reedy Point, Philadelphia, Chesapeake City, and Town Point. A series of programs were written for generating the required input data files as well as graphically displaying model results and field data.

## Forcing Functions

To obtain realistic predictions from a numerical model, the external forcing variables must be specified correctly. The forcing database to drive the CH3D-WES code includes: (a) water-surface elevations at the open boundaries, (b) freshwater inflow from the tidal limit of the river, (c) surface wind stress, and (d) the initial salinity distribution plus time-varying salinities at the open boundaries.

### Free-surface elevation

In this system, two open tidal boundaries are considered. Figures 5(a)-(c)

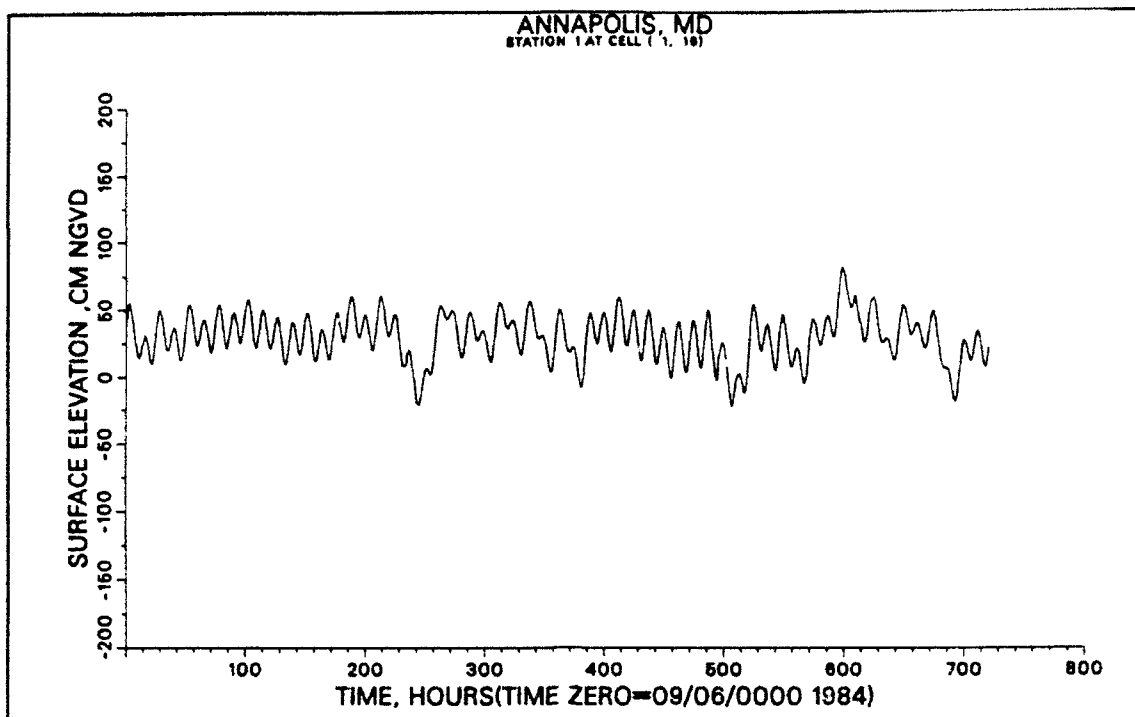


Figure 5a. Recorded tide at Annapolis (hrs)

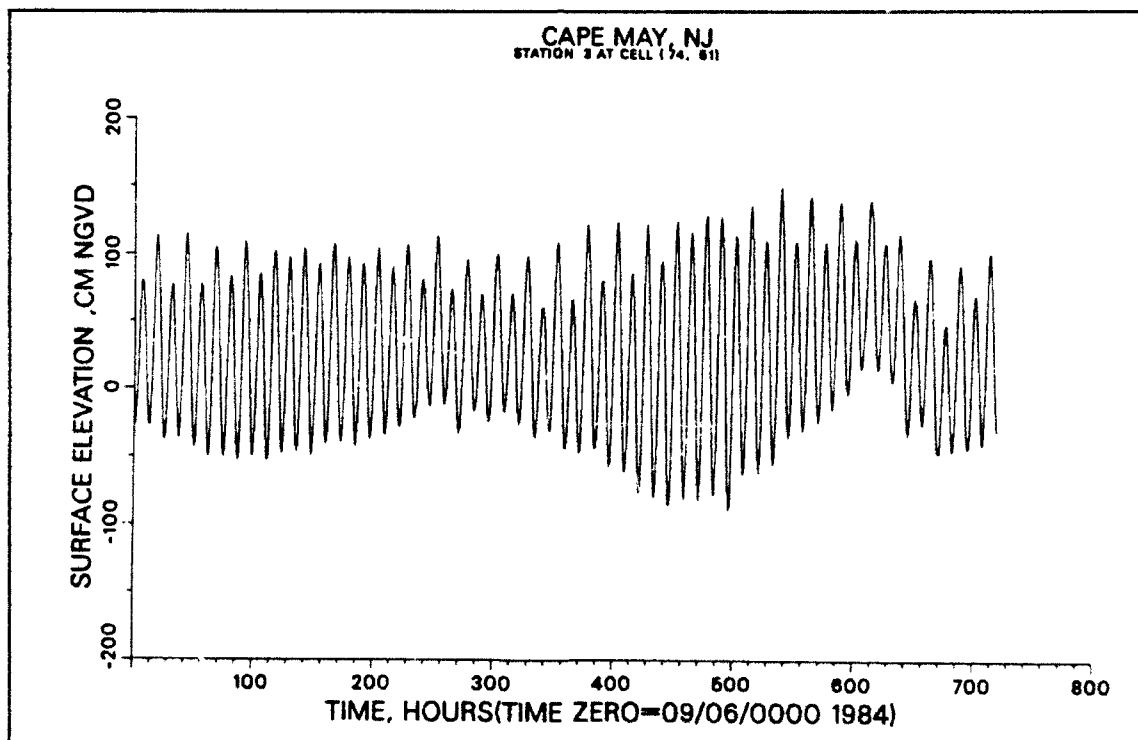


Figure 5b. Recorded tide at Cape May (hrs)

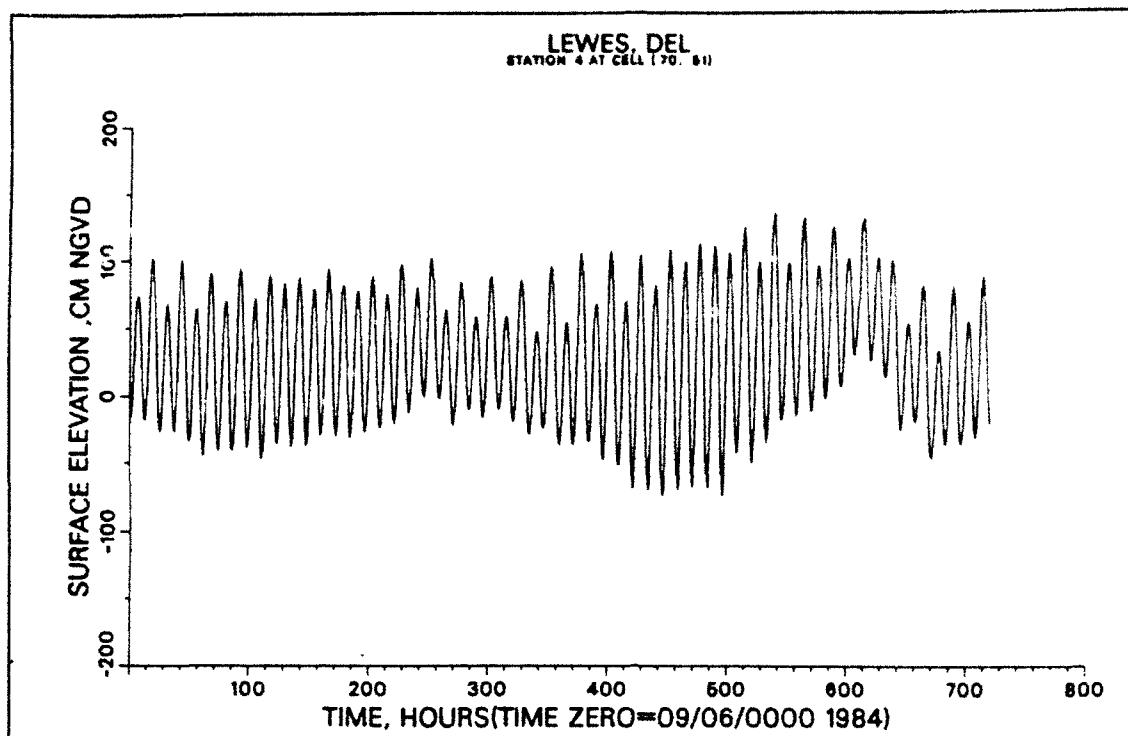


Figure 5c. Recorded tide at Lewes (hrs)

show hourly month-long tidal fluctuations for these forcings. The Delaware Bay entrance has a strong semi-diurnal and neap-spring pattern. A mixed and damped tide is found at Annapolis. To prescribe the variations of tide over the wide Delaware Bay entrance, free-surface elevations between Cape May and Lewes were interpolated. Cubic spline interpolation was used to capture extreme values. As previously noted, the arrival times of the Chesapeake Bay and Delaware Bay tides at the west and east ends of the C&D Canal are separated by approximately 10 hrs.

### Freshwater runoff

The major contributions of freshwater into the system are the Delaware, Schuylkill, and Susquehanna Rivers. These inflows for September 1984 were obtained from USGS gages and are shown in Figures 6(a)-(c). The Schuylkill River's runoff is combined with that from the Delaware River at Trenton and inserted into the model as a single source. The daily averaged runoff values are linearly interpolated to provide data at each time step. The effects of local contributions from other rivers and tributaries were considered to be negligible.

### Surface wind stress

Surface wind stress was calculated using hourly wind data at the Baltimore-Washington International Airport (BWI) and Wilmington stations. These data

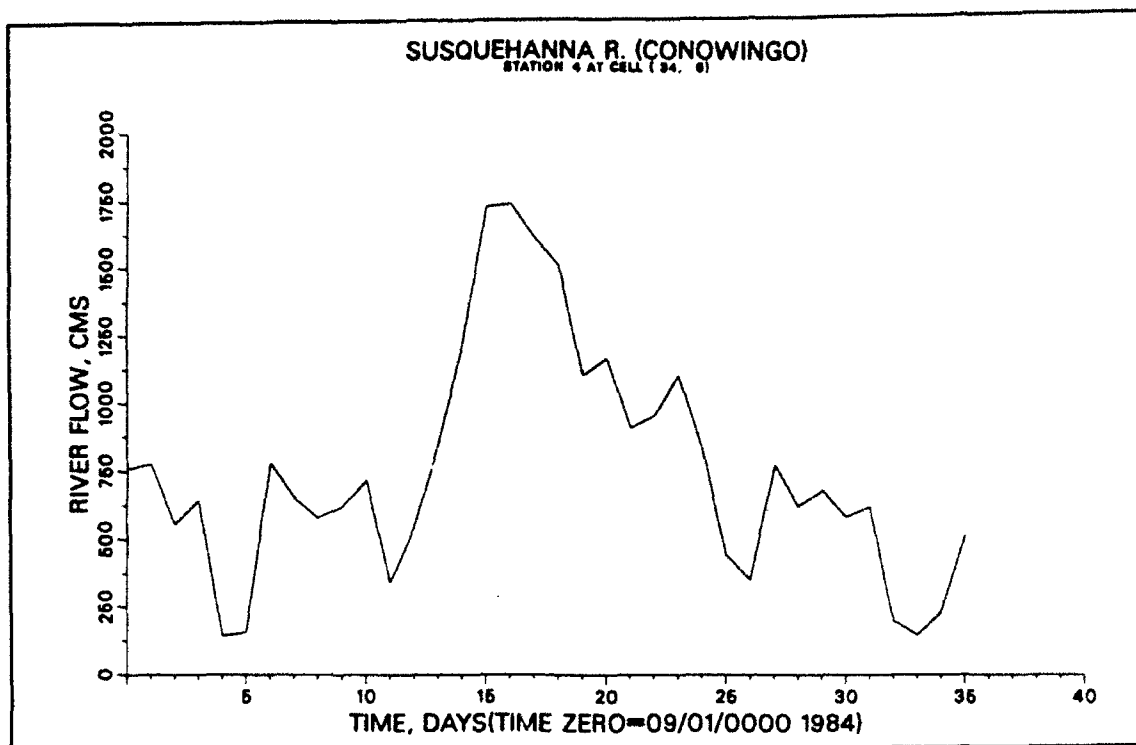


Figure 6a. Freshwater inflow from Susquehanna River

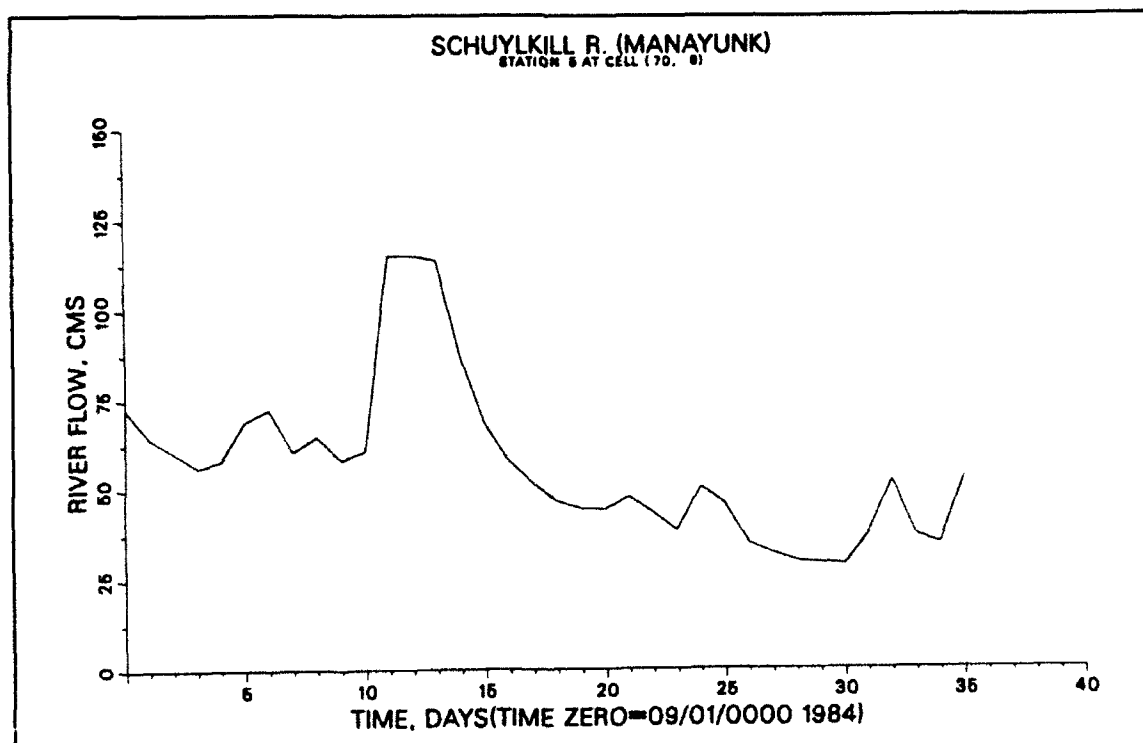


Figure 6b. Freshwater inflow from Schuylkill River

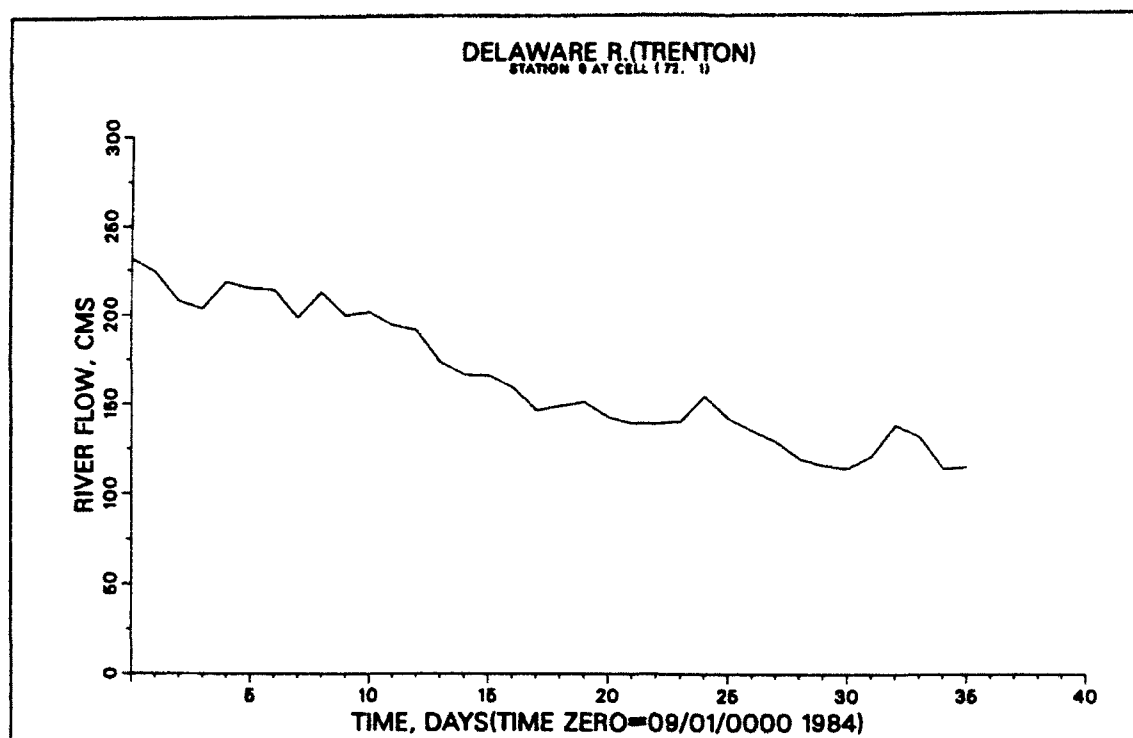


Figure 6c. Freshwater inflow from Delaware River

were provided by the National Climatic Data Center, Ashville, NC and are illustrated in Figures 7(a)-b). Over-water winds were calculated according to Hsu's (1986) formula.

$$U_{sea} = 1.62 + 1.17 U_{land}$$

This formula suggests a simple dimensional relation between the wind velocity over the sea and over land. In this study, the wind field over the Upper Chesapeake Bay was prescribed by the BWI data and the Delaware Bay wind field was represented using the Wilmington data. The wind field over the C&D Canal was obtained by an interpolation between these two regions.

### Boundary and initial salinity distributions

Time-varying salinity data at all the grid points on the ocean boundaries are required. Discrete data collected near the surface and near the bottom were used to generate the required boundary profiles. Bi-weekly information exists near the Bay Bridge for the September 1984 period. However, no Delaware source salinity data from the NODC (National Oceanographic Data Center) tape (NOS 84-85 Delaware Bay circulation study) were available during this period. DRBC's bi-weekly to weekly Delaware Bay salinity data could be used for model verification, but they were not useful for generating initial and

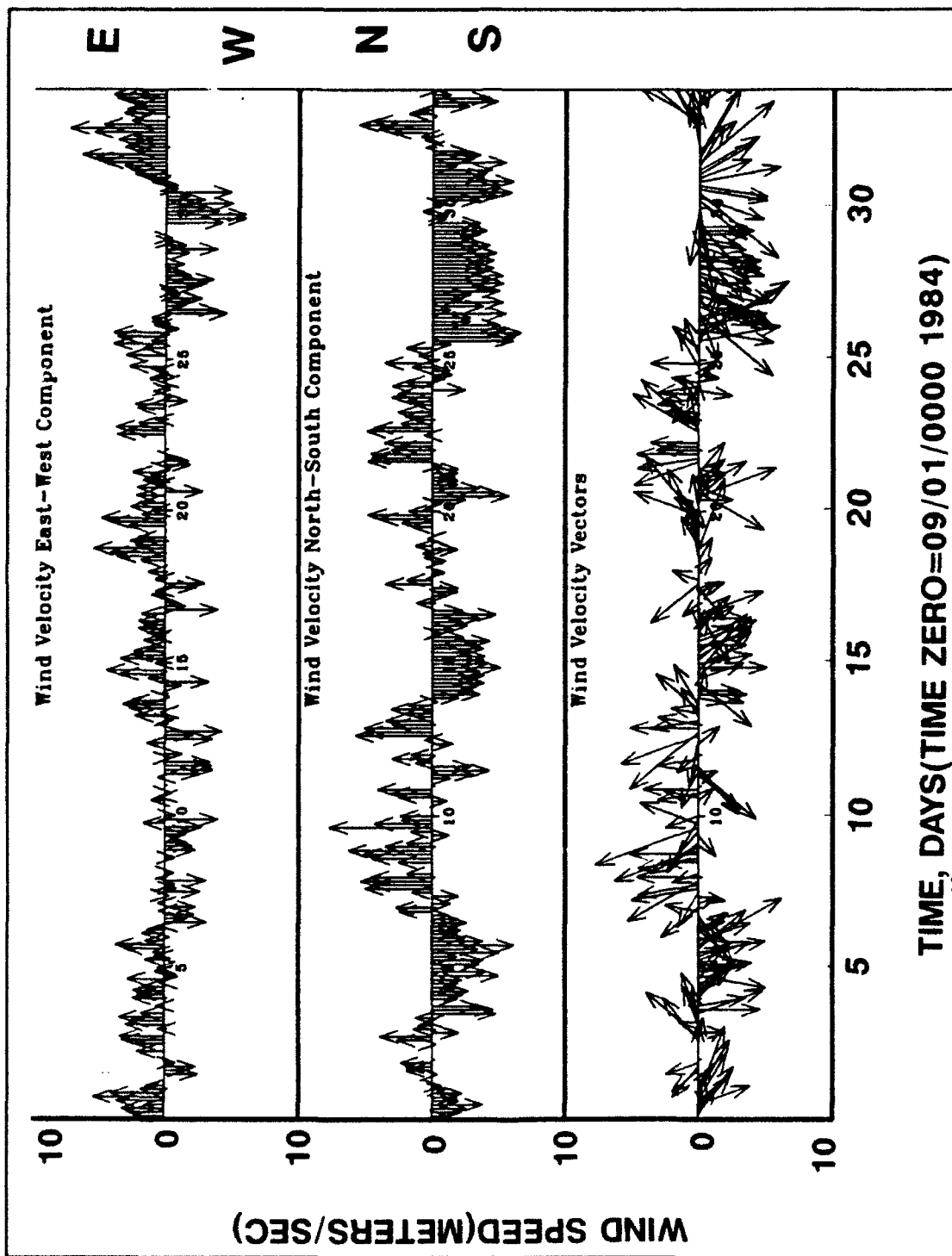


Figure 7a. Wind at Baltimore-Washington Airport, Maryland

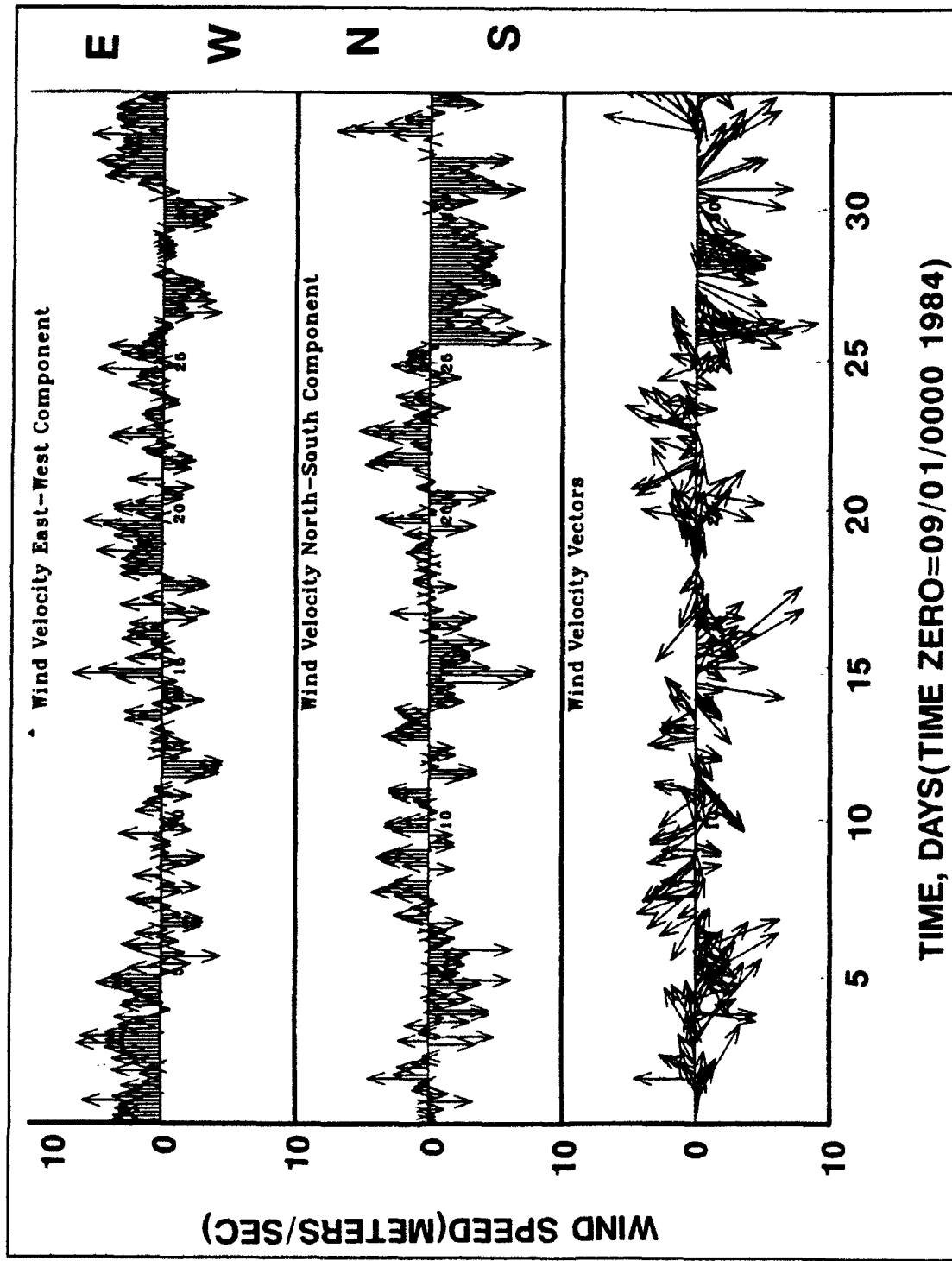


Figure 7b. Wind at Wilmington, Delaware

boundary conditions. As an approximation, available data at the Chesapeake Bay entrance were used for the Delaware source salinity. The values are shown in Table 1.

<b>Table 1</b> <b>Salinity Boundaries (ppt) Used for Monthly Simulation</b> <b>(9/6/1984 - 10/5/1984)</b>				
	Delaware Bay Entrance		Chesapeake Bay Bridge	
Date	Near Surface	Near Bottom	Near Surface	Near Bottom
8/22/84	26.35	29.38	3.68	6.70
9/01/84	28.15	30.12	4.96	8.24
9/11/84	28.20	28.50	6.24	9.78
9/21/84	26.10	26.55	8.24	10.47
10/01/84	25.55	26.60	8.53	10.89
10/11/84	25.80	27.80	8.40	10.05

The initial salinity distribution was obtained by interpolation/extrapolation of known values at particular points. The resulting field was then smoothed using a three point smoothing equation.

## Verification of the Homogeneous Model

### Harmonic tidal test

The model was initially tested by analyzing the propagation of tidal waves. The  $M_2$  (principal lunar semi-diurnal) constituents were prescribed at both boundaries and the amplitude and phase between model results and the harmonic constants at several interior points were then compared. The model was run for 10 tidal cycles without density effects. After adjusting the bottom drag and system coefficients, e.g. minimum values of vertical eddy viscosity, the water surface elevation agreement was reasonable, however, predicted tidal currents in the canal were extremely high. In addition, model tidal phase led the prototype by about one hour at most locations in the C&D canal. Additional adjustment of bathymetry and bottom drag coefficients did not improve velocities adequately.

### Inset model test of the canal

An inset model was constructed by extracting computational cells between Old Town Point and Reedy Point. The actual observed tide records were used at each end of the canal inset grid for boundary conditions. Since both entrances of the canal were forced, the accuracy of predicting interior surface elevation was improved. A series of inset grid tests were conducted by examining the sensitivity of results to wind stress, non-linear terms in the



equations of motion, the entrance loss term at both ends of the canal, the bottom drag coefficients, and the effect of tidal datums. The canal hydrodynamics were found to be the most sensitive to the tidal datum plane.

An unknown datum level at Old Town Point (data source from University of Maryland) was adjusted until good agreement between field measurements and computational results was obtained. This test showed that the accuracy of the relative head difference was a key element in correctly computing tidal flows in the canal. The inset model was run for twenty tidal cycles with the last fifteen cycles used for comparison. Highly accurate currents in all three layers at Summit Bridge were obtained after making the datum correction of about 15 cm, and providing reasonable bottom drag coefficients.

### Full grid hydrodynamic test

The information gained from the inset grid tests was extended to verify the full grid model. The tidal data for this study came from three different sources. They consisted of corrected NGVD values at Annapolis and Havre De Grace, uncorrected NGVD values at the Delaware's tide gauges, and no reference level at Town Point (data source from University of Maryland). Obviously, the verification effort required datum consistency. To provide a consistent vertical datum, all gauges were initially referenced to the local 1984 record's mean tide level. However, local mean tidal levels vary from location to location. Therefore, using mean tide level as the datum introduced error in the relative head difference between the two end tidal boundaries and resulted in canal currents being as much as three times their true values. The tidal datums were then set to local corrected NGVD (Table 2). This was accomplished by subtracting the local NGVD correction from the raw tidal data. After these corrections were made, the improvement in canal velocity verification was dramatic. Consistency in measuring NGVD is essential when employing field tidal data to drive numerical models.

<b>Table 2</b> <b>Datum<sup>1</sup> of Tidal Gauges in the C&amp;D Canal System (feet)</b>			
<b>Station</b>	<b>MLW</b>	<b>MLLW</b>	<b>NGVD</b>
Annapolis	4.54	4.30	4.46
Harve De Grace	6.33	6.08	6.58
Cape May	2.30	2.14	4.14
Lewes	2.67	2.51	4.23
Reedy Point	1.23	1.04	3.54
Philadelphia	3.74	3.55	5.84
Chesapeake City	3.15	2.81	3.90
Town Point	3.53	3.31	-
<sup>1</sup> from National Ocean Service, NOAA.			

## Final Month-Long Verification

After the homogeneous model was verified, input files were set up for month-long verification runs with salinity computed. The final values for the bottom drag coefficient ranged from 0.0025 to 0.0040 in the Delaware Bay, and were 0.0050 in the C&D Canal and 0.0025 in Upper Chesapeake Bay. The model was run from September 1, 1984 to October 5, 1984 using a one minute time step. The salt field was fixed for the first 5 days. Computed results were then saved at a half-hour interval for the next thirty days for verification comparisons. Each run required about 4 hours CPU time on a Cray Y-MP supercomputer.

### Surface Elevation

Comparison of model results and field data at five interior gauges are shown in Figure 8(a) - (e). In general, the agreement between numerical predictions and observed data is good with regard to both amplitude and phase. The largest phase error in computed results occurs at Havre de Grace. This area is close to Conowingo Reservoir, and the reflected tidal wave combined with the new wave arrival may cause the occurrence of a standing wave. In addition, the model used 10 feet to represent the mean water depth of the Susquehanna Flats, which are actually shallower. The Reedy Point and Philadelphia gauges exhibit fair agreement. Excellent agreement is found at Town Point while the Chesapeake City gauge comparison shows some phase error.

### Tidal currents

Data for only two current stations were available for this time period. Figures 9(a) - (c) show comparisons at the 10 meter, 7 meter and 4 meter depths (below surface) at Summit Bridge. The excellent match illustrated in these plots indicates the model's capability of reproducing flow transport in the canal. The two components of the current at Arnold Point, (see Figure 1b) are presented in Figures 9(d) - 9(e). One would conclude from the results in Figure 9d that perhaps the velocity components being compared are not entirely aligned. Detailed refinement of local roughness and water depth might also improve these results.

### Salinity regime

The most difficult part of the verification was to accurately reproduce the salinity throughout the modeled area for a dynamic period of the year, especially since the vertical profiles at the boundaries are uncertain. However, extremely good results were obtained at Summit Bridge. Figures 10(a) - (c) are presented for the near-bottom-layer (10 m, layer 6), the mid-depth-layer (7 m, layer 8) and the near-surface-layer (4 m, layer 10). At the mid-depth-layer, the salinity is underestimated by about 1.5 ppt between days 10 and

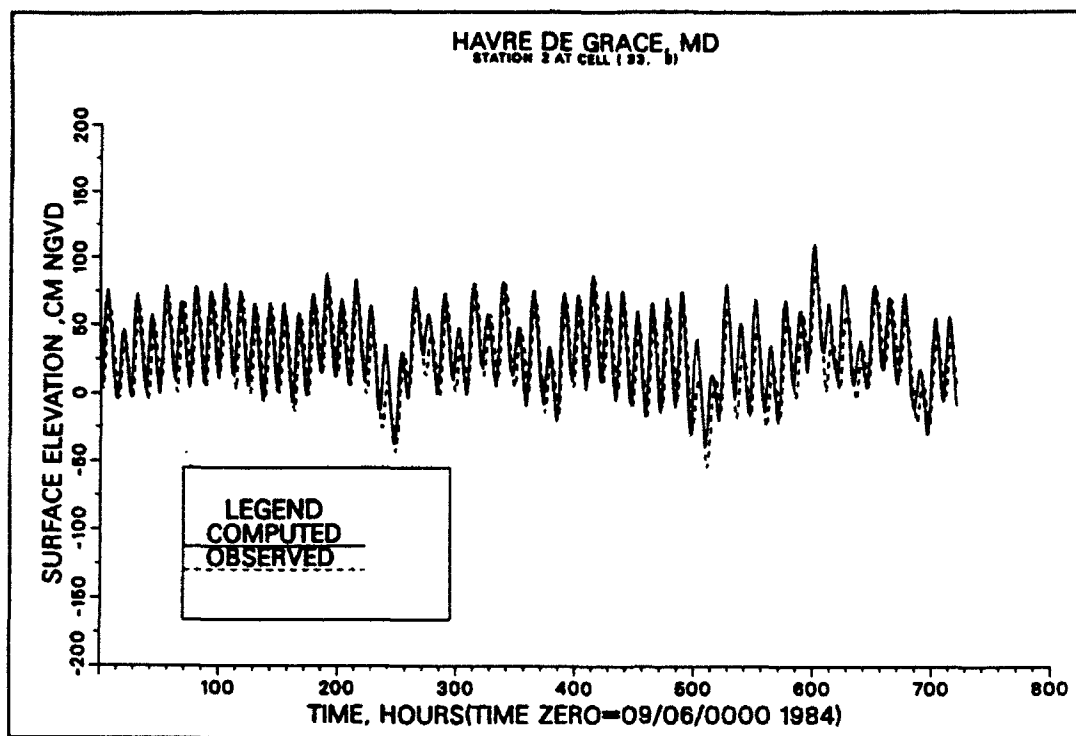


Figure 8a. Computed versus recorded tide at Havre De Grace

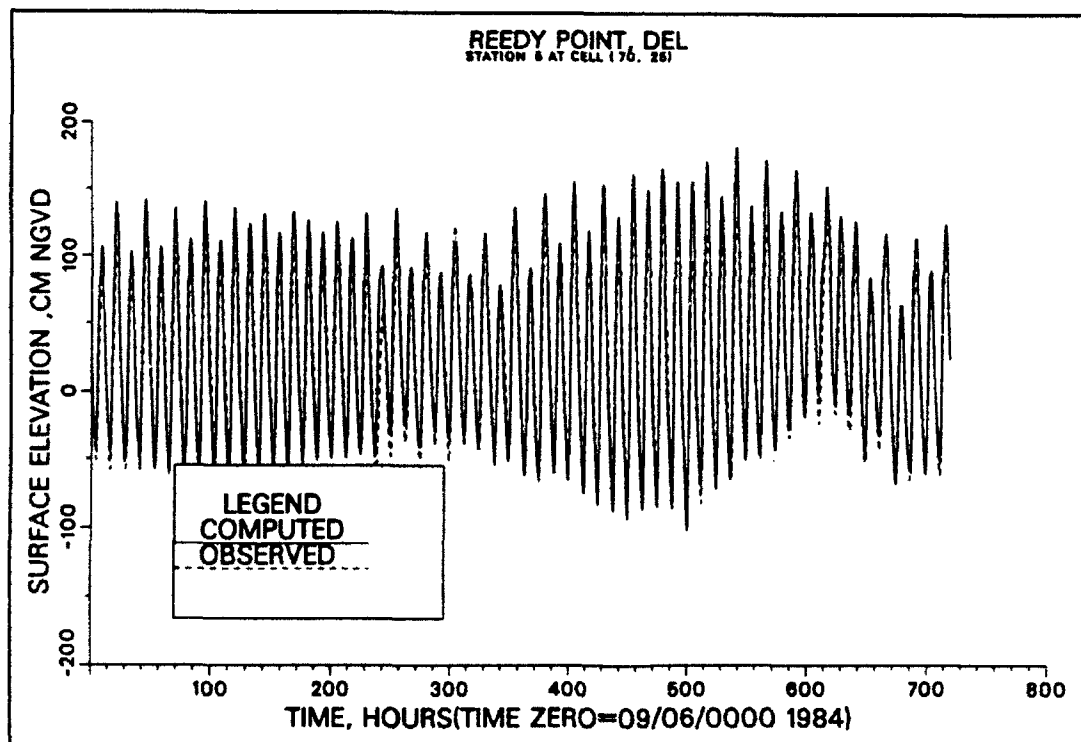


Figure 8b. Computed versus recorded tide at Reedy Point

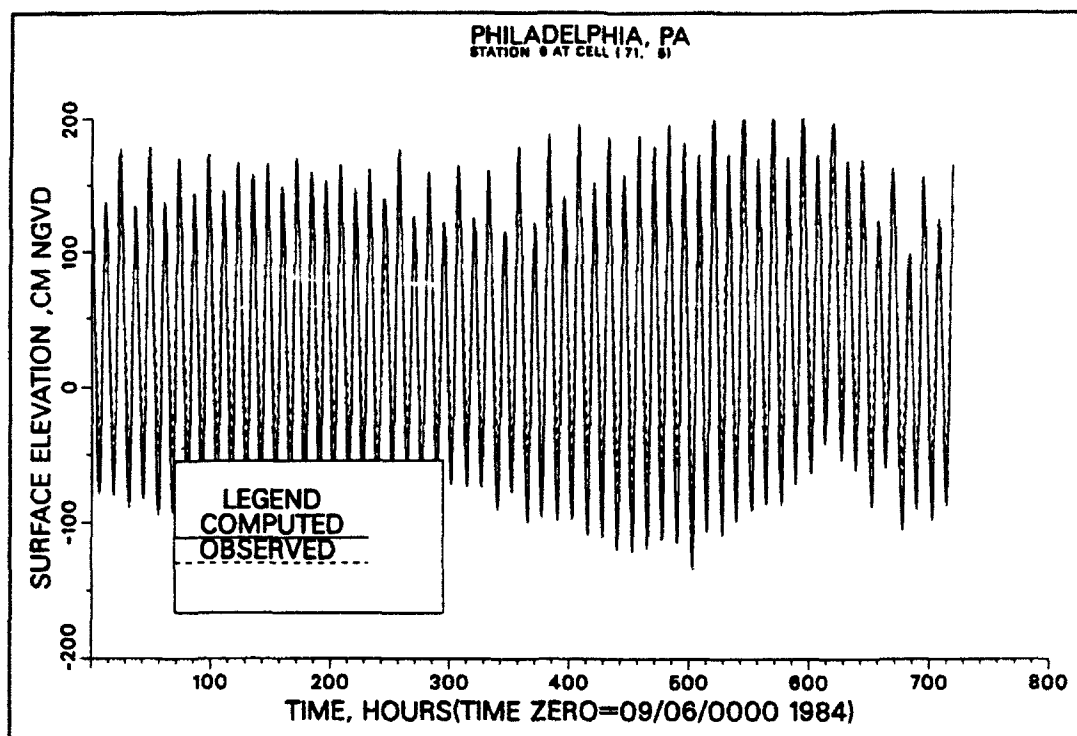


Figure 8c. Computed versus recorded tide at Philadelphia

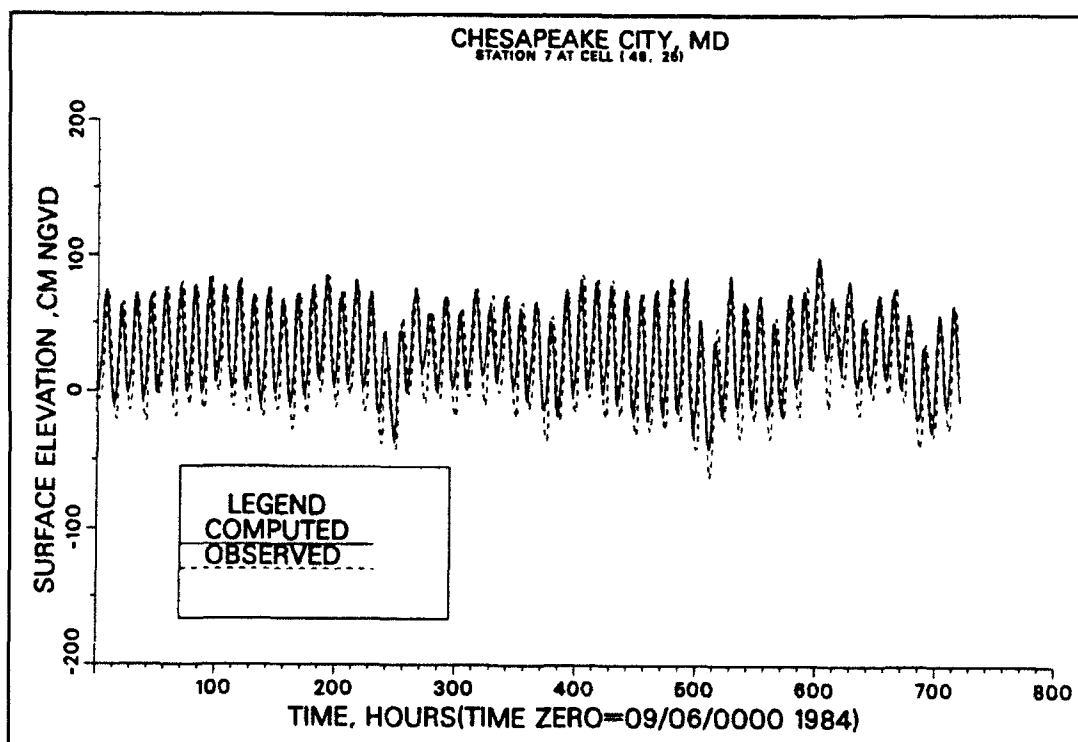


Figure 8d. Computed versus recorded tide at Chesapeake City

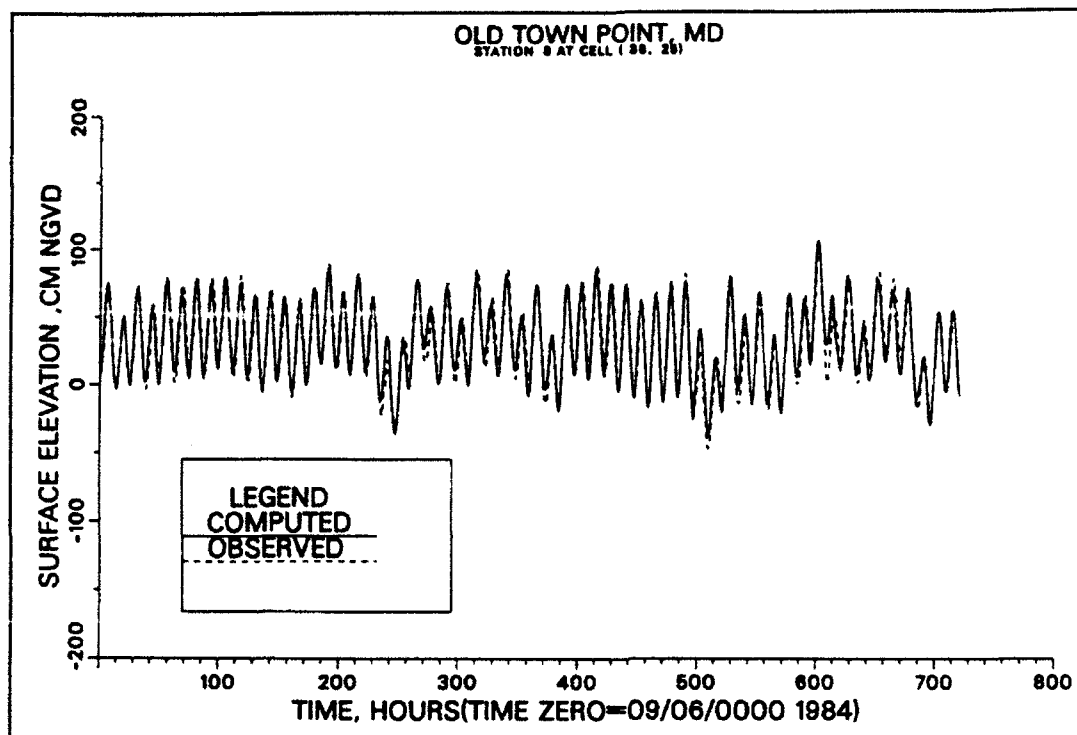


Figure 8e. Computed versus recorded tide at Old Town Point

17 (hours 90 and 130). However, excellent agreement is again obtained after this period. Two gauges in Upper Chesapeake Bay (Figure 10(d) - (e)) also show fairly good results. Differences could probably have been reduced if field data existed to allow a more realistic representation of the open boundary and initial conditions. The salinity at Reedy Point (Figure 10(f)) was reproduced by the model fairly well, especially over the last half of the simulation period. A weak tidal oscillation occurred in the salinity at this location during the first half of the simulation. This may be related to the prescribed initial salinity field.

### 3-D Tidally Averaged Circulation

Monthly averaged velocity vectors were computed for each layer of the model. Figure 11 and Figure 12 show these currents for the near-surface (layer 11) and near-bottom of the canal (layer 6), respectively. The middle part of Chesapeake Bay forms a nodal point in tidal circulation. During this period of time, Delaware Bay contributed both near-surface and near bottom, non-tidal flow to Chesapeake Bay through the canal. Salinity intrusion along the main channel near the bottom occurs in both lower Delaware Bay and upper Chesapeake Bay.

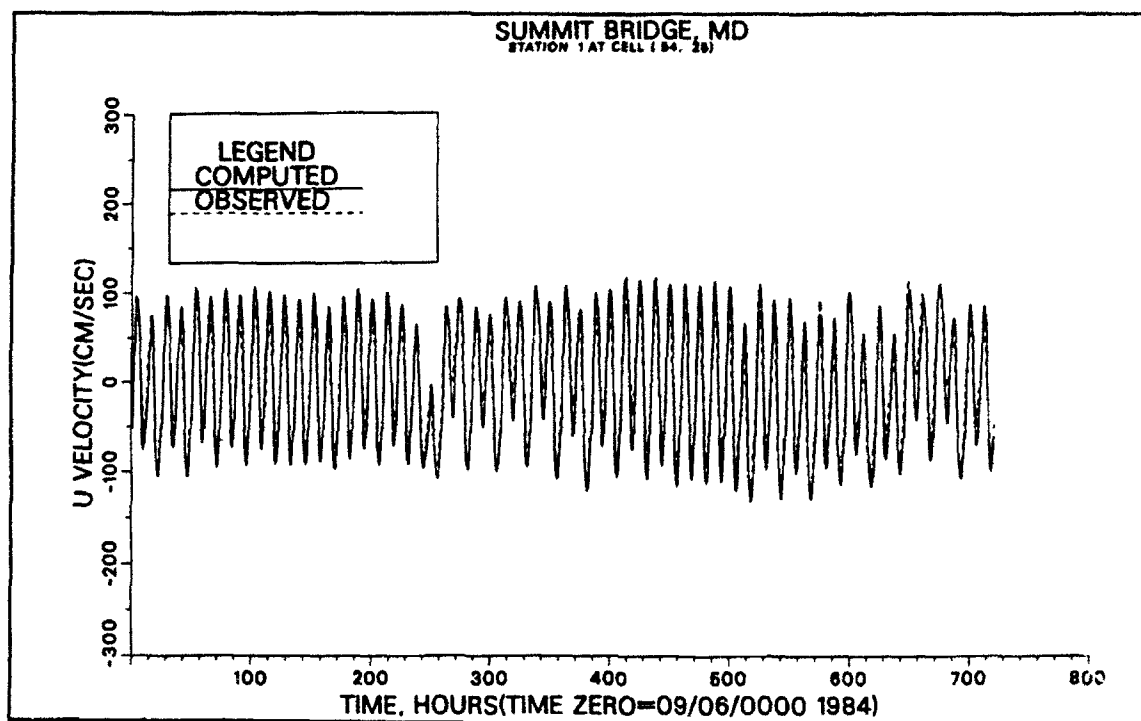


Figure 9a. Computed (solid line) versus recorded (dashed line) velocity at Summit Bridge (10 m)

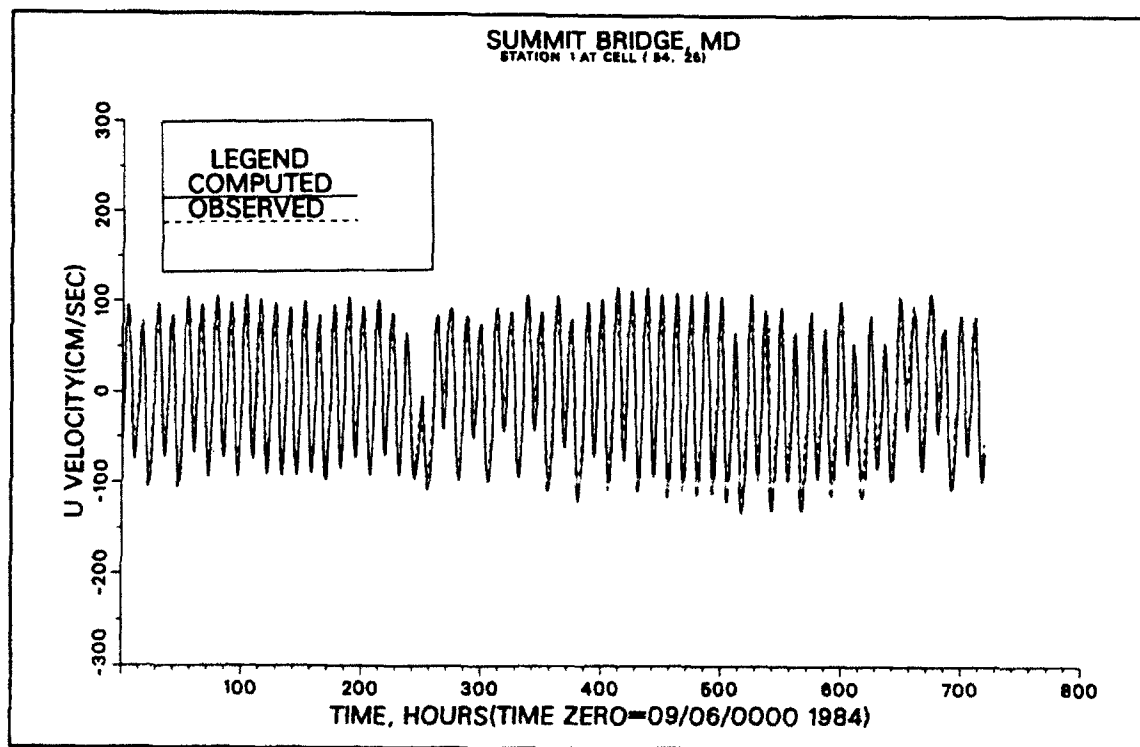


Figure 9b. Computed versus recorded velocity at Summit Bridge (7 m)

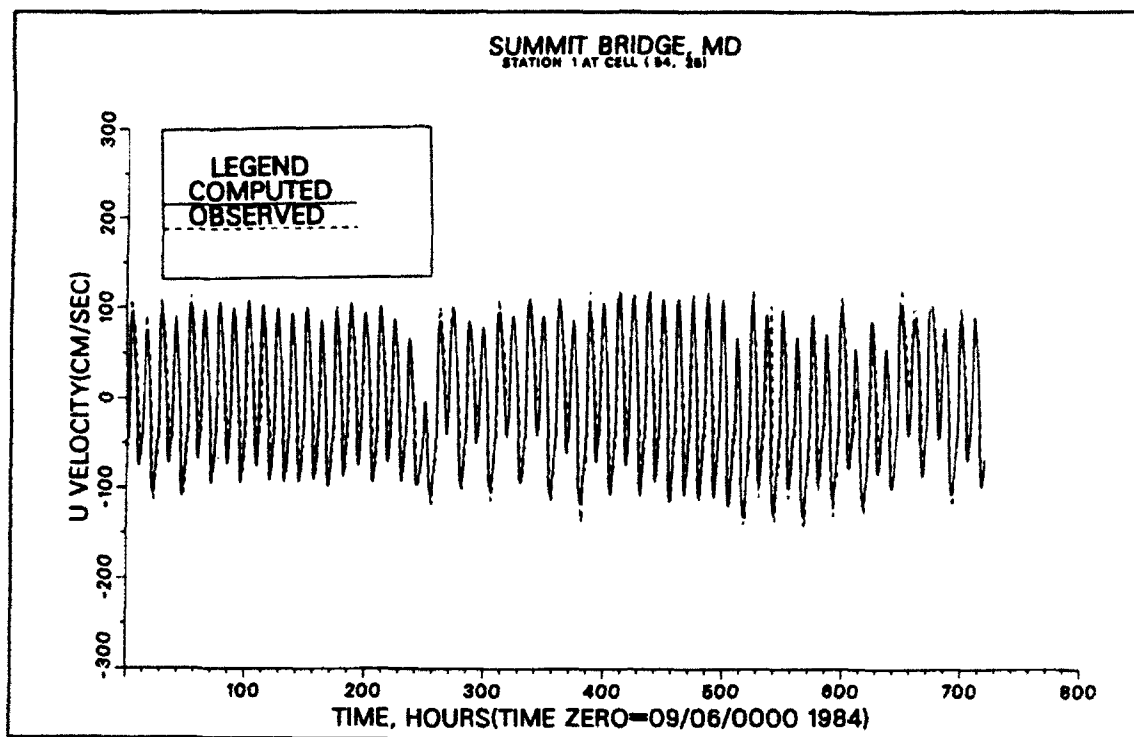


Figure 9c. Computed versus recorded velocity at Summit Bridge (4 m)

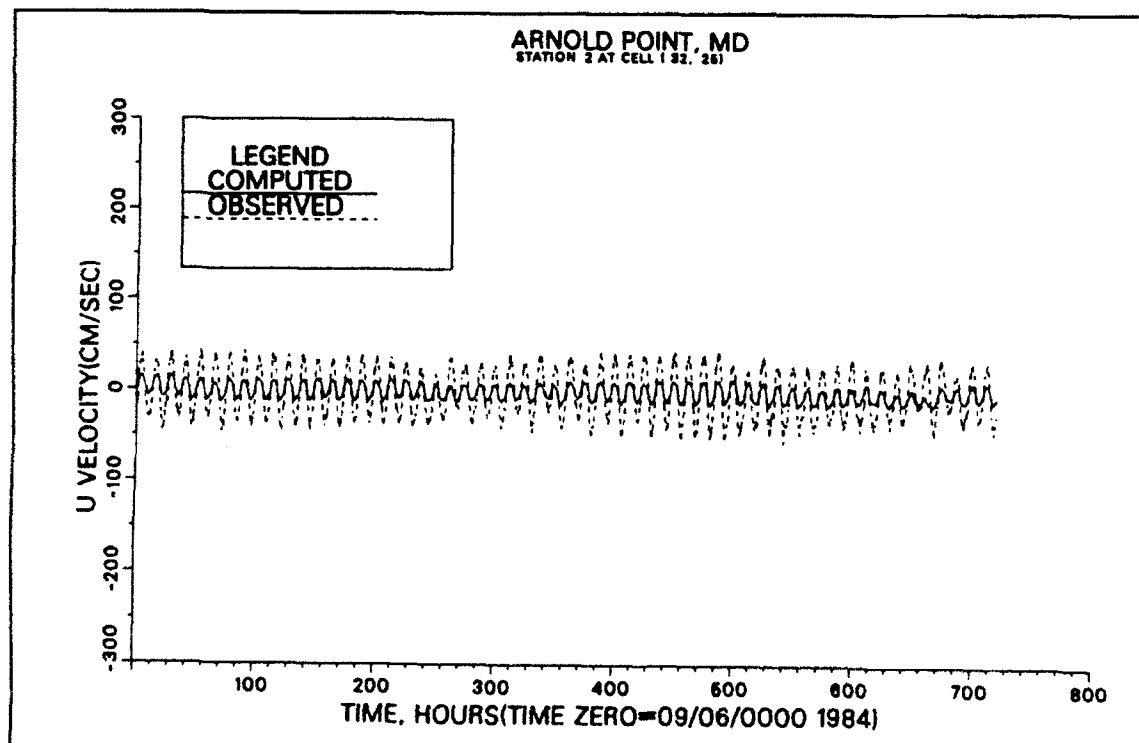


Figure 9d. Computed versus recorded velocity at Arnold Point (4 m)

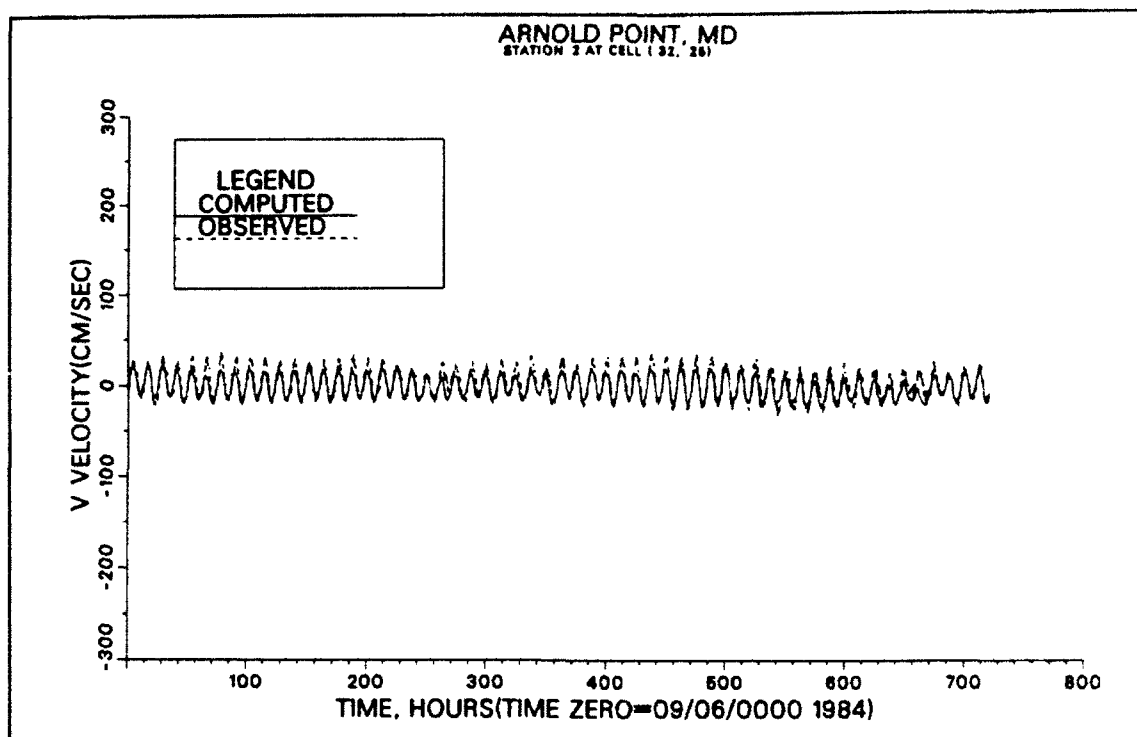


Figure 9e. Computed versus recorded velocity at Arnold Point (4 m)



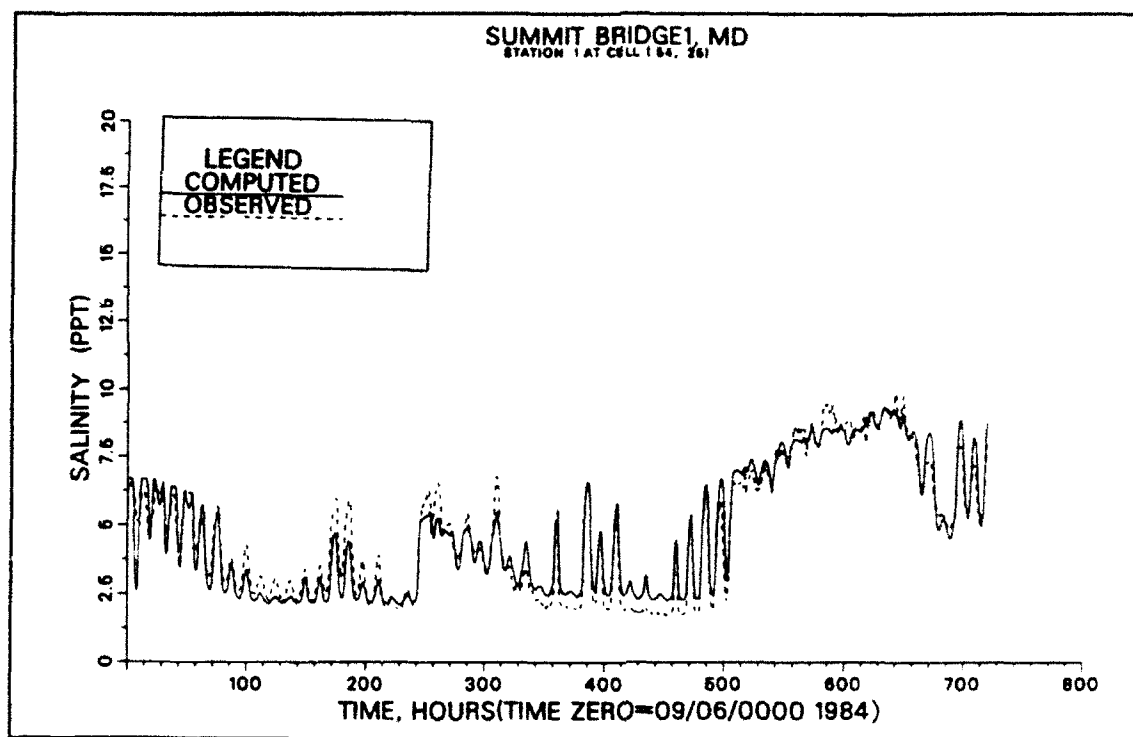


Figure 10a. Computed (solid line) versus recorded (dashed line) salinity at Summit Bridge (10 m)

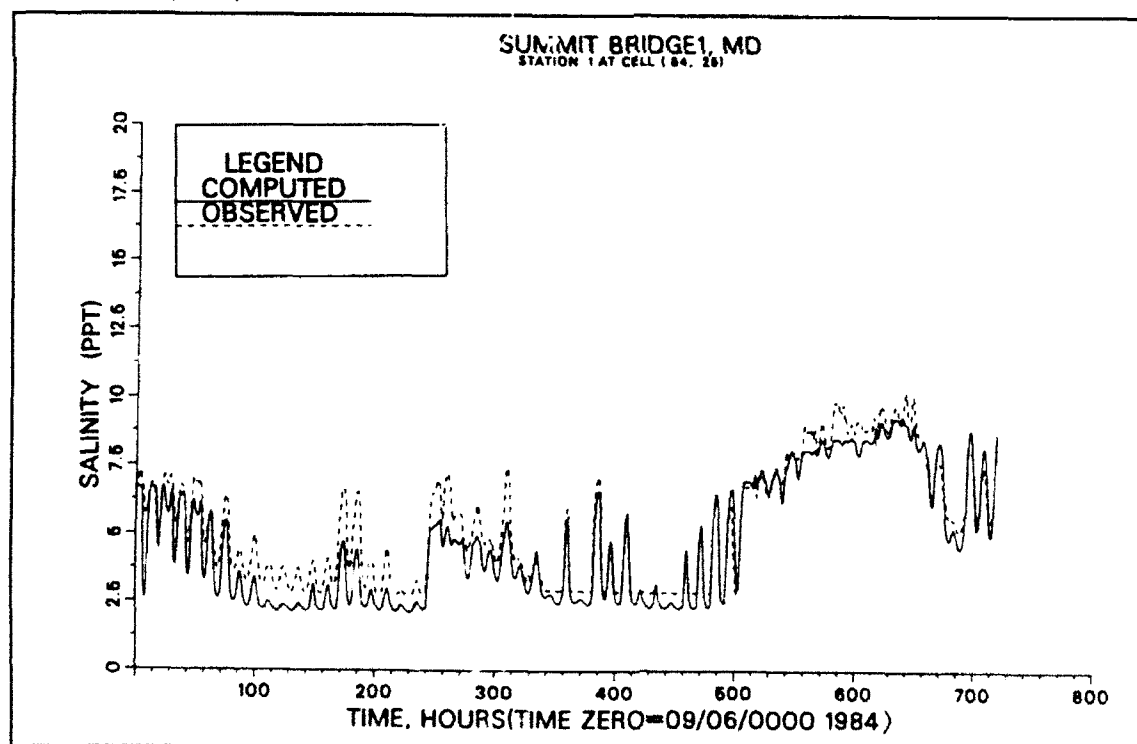


Figure 10b. Computed versus recorded salinity at Summit Bridge (7 m)

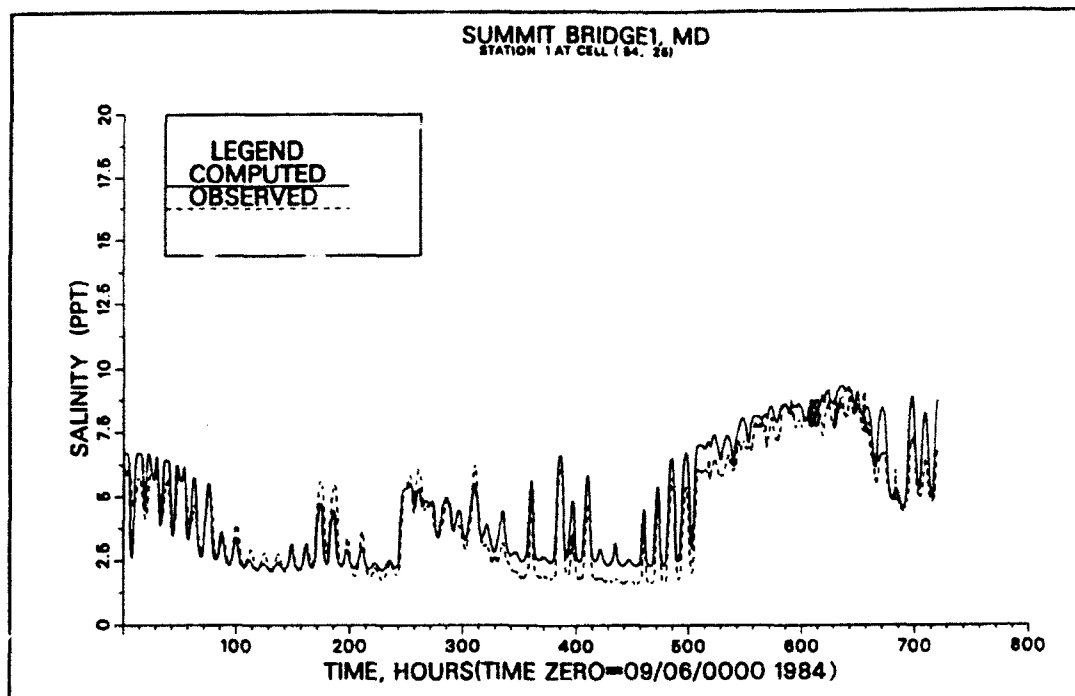


Figure 10c. Computed versus recorded salinity at Summit Bridge (4 m)

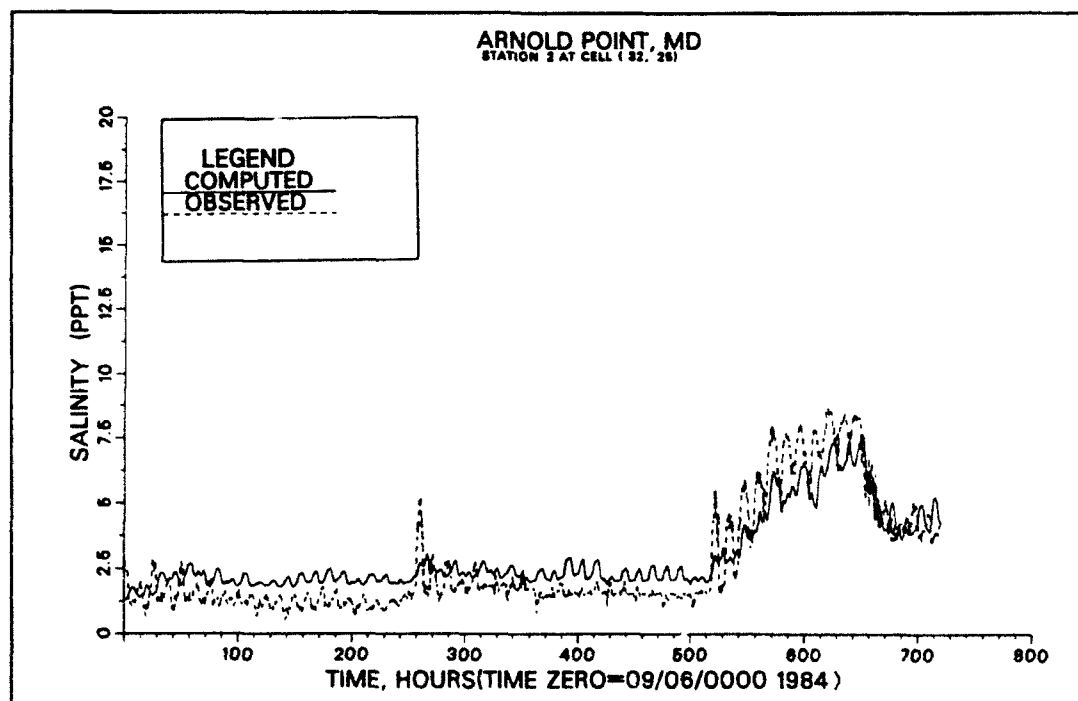


Figure 10d. Computed versus recorded salinity at Arnold Point (4 m)

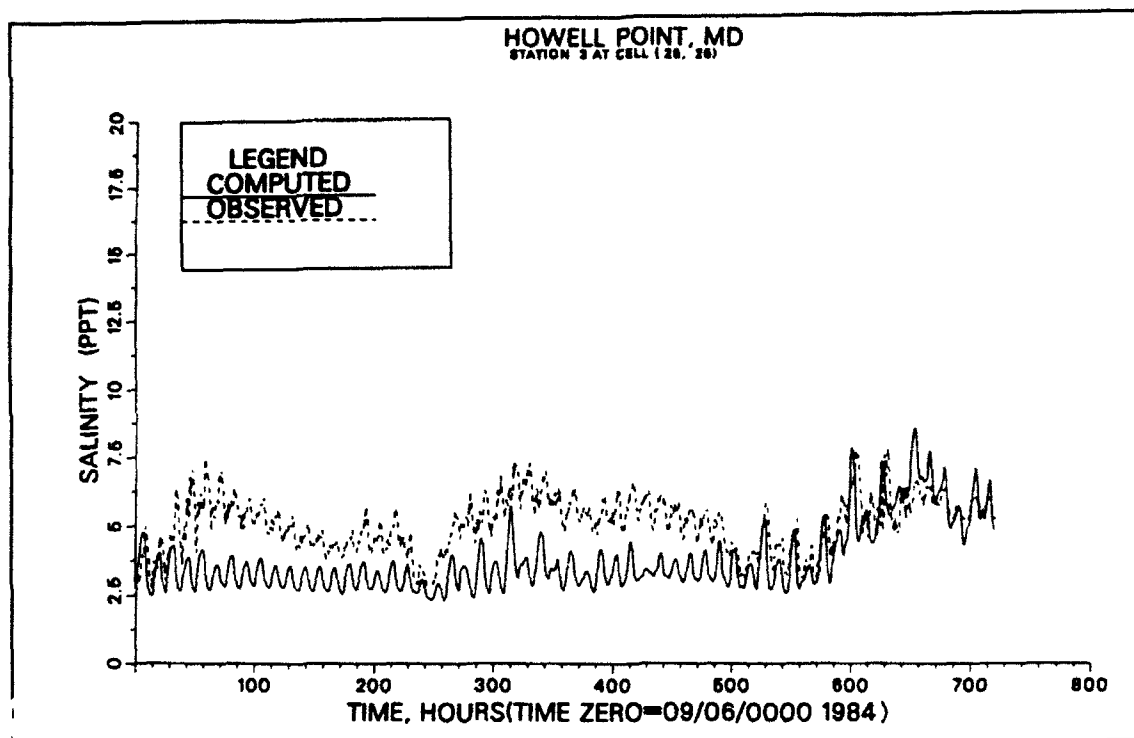


Figure 10e. Computed versus recorded salinity at Howell Point (5.5 m)

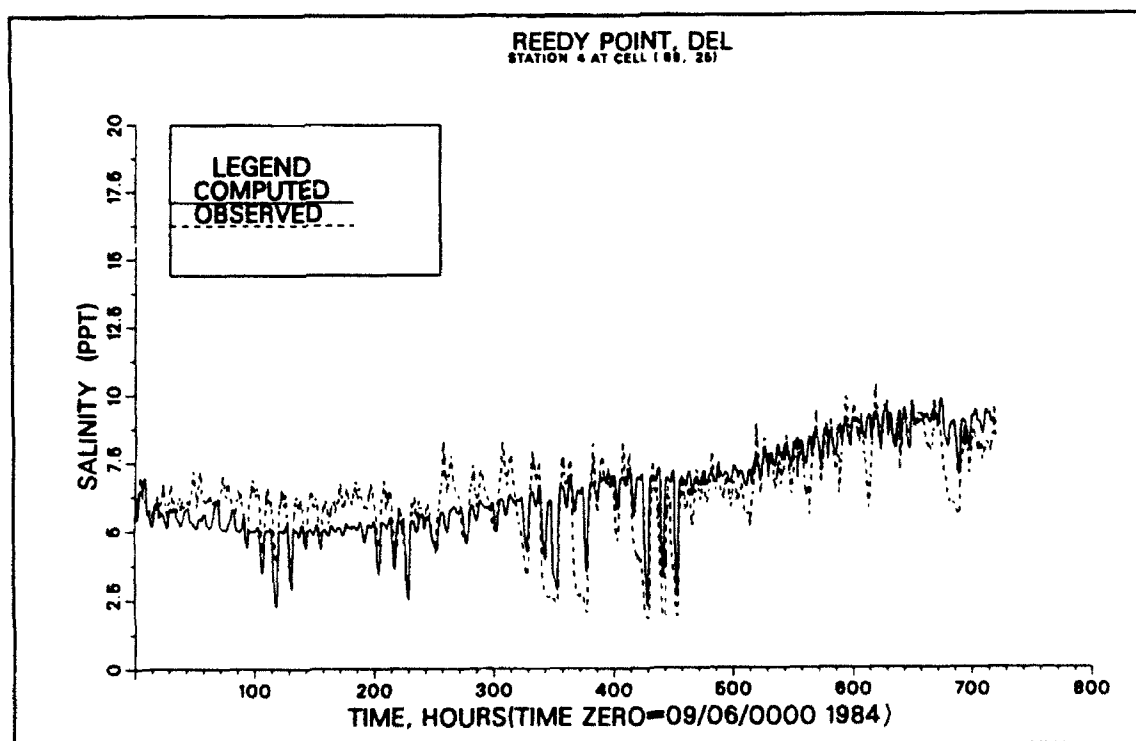


Figure 10f. Computed versus recorded salinity at Reedy Point (2.5 m)

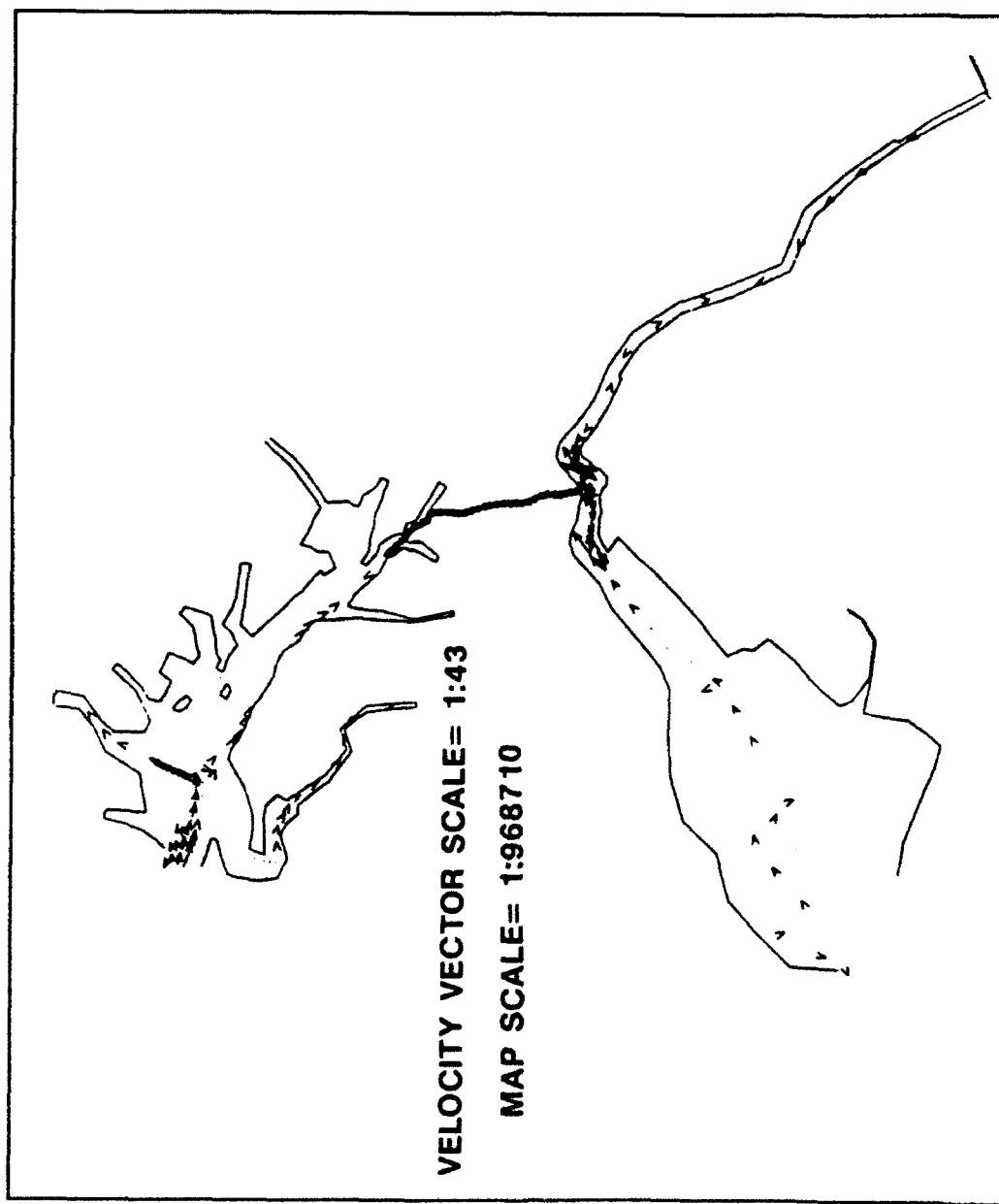


Figure 11. Computed monthly averaged tidal circulation (Layer 11, 2.3 m) (near surface) strong westerly netflow in the C&D canal was found

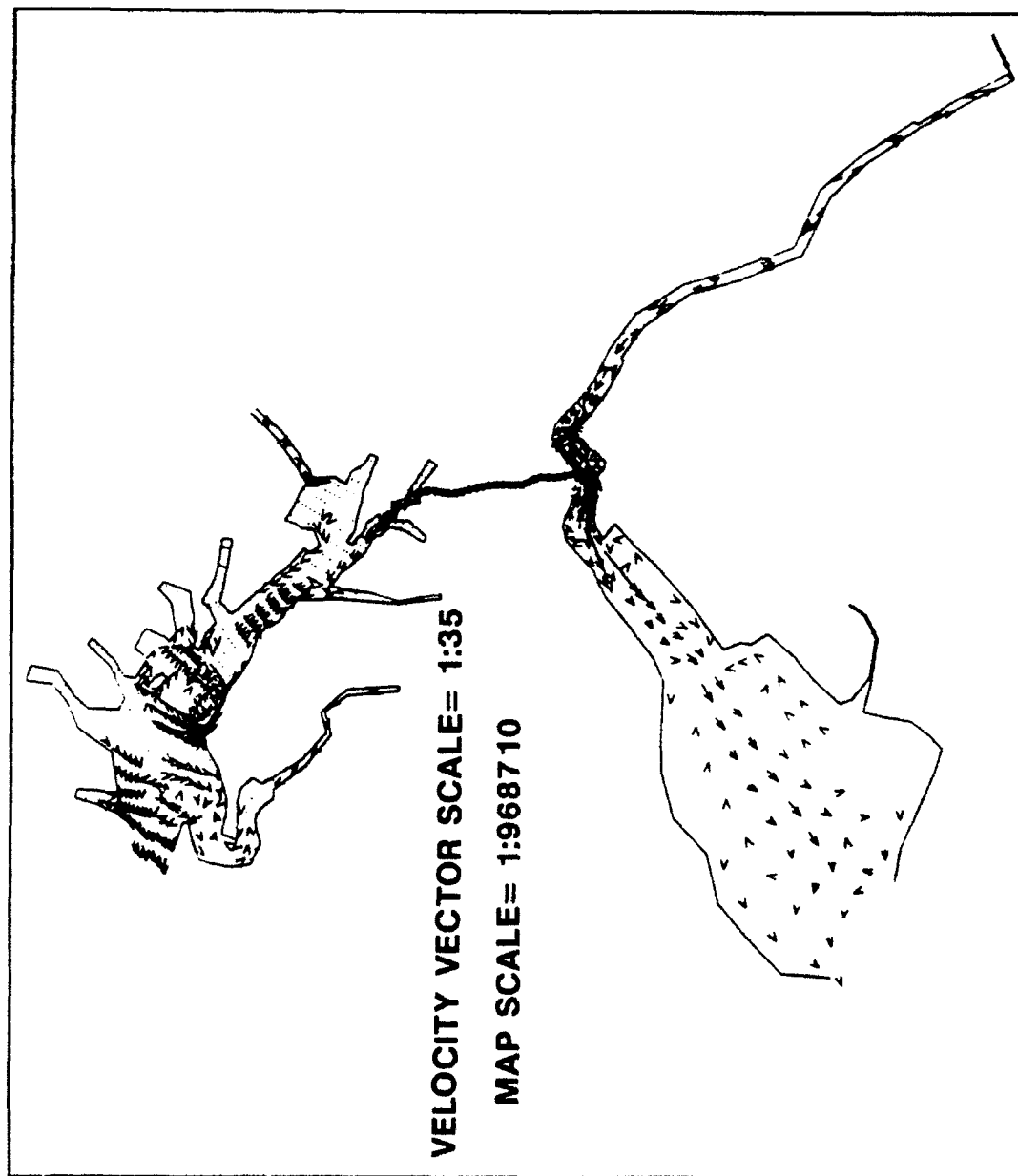


Figure 12. Computed monthly averaged tidal circulation (Layer 6, 11.3 m) (near bottom)

## 4 Net Transport Due to Channel Deepening

---

A verified numerical model, especially a 3-D model, can be used as a tool to examine many problems, such as the estimation of net transport for a range of channel depths. To compute transport through the C&D Canal, the area of each computation cell for a particular cross-section was multiplied by the current speed in the channel direction and then integrated over time. Average transport was obtained by integrating the flow field over time from slack-before-ebb flow to the following slack-before-ebb flow and dividing by the elapsed time. The elapsed time for each intra-tidal calculation varied with the duration of that tidal cycle. The thickness of the top layer in the model was determined by the surface elevation whereas the thickness of all other layers was constant. Cumulative transport was averaged over the entire record from the first occurrence of "slack before ebb flow" to the end of the particular tidal cycle. (Rives and Pritchard, 1978). The salt transport was calculated as the area of each computation cell in a cross-section multiplied by the current speed and salinity concentration, and then integrated over time.

Attempts to define relationships between discharge (volume transport),  $Q$ , and head difference,  $\Delta H$ , between the water level at two boundaries of the canal were made. Since the length of the C&D Canal is small compared to the tidal wave length, the water surface slope in the canal is essentially linear. The flow in the canal is driven by this linear grade line. Therefore, previous investigations have proposed linear relationships to describe the nontidal flow in the canal in terms of the difference of mean tide level between the two end boundaries. In this study, the model outputs (40-foot channel base run) of surface elevations at Old Town Point and Reedy Point, and tidal currents and surface elevation at Summit Bridge were used to identify this relationship. Figure 13a shows the head difference and Figure 13b shows inter-tidal transport during this month long simulation. The response time (lag) of head difference on inducing flow at Summit Bridge was considered in the ratio of volume transport to head difference computation. The highest correlated condition (Figure 13c) was found by taking a 1.5 hours phase lag between the transport and the head difference series. This infers that the salinity response to gravity flow is delayed approximately 1.5 hours in the canal system. The positive sign indicates an eastern flow and the negative sign corresponds to a western flow. Note that the spikes indicate the short duration of "slack water" during which time the current changes direction. Although some extreme

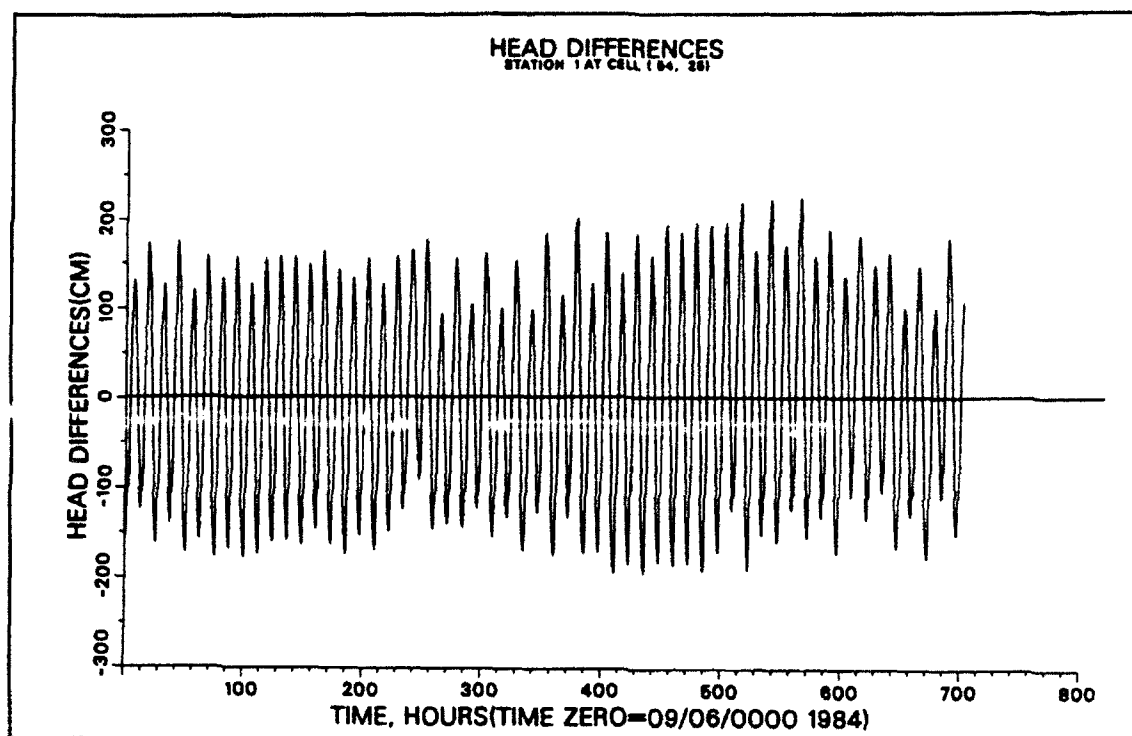


Figure 13a. Computed surface elevation differences  $\eta_{OT}$  (Old Town Point) -  $\eta_{RT}$  (Reedy Point)

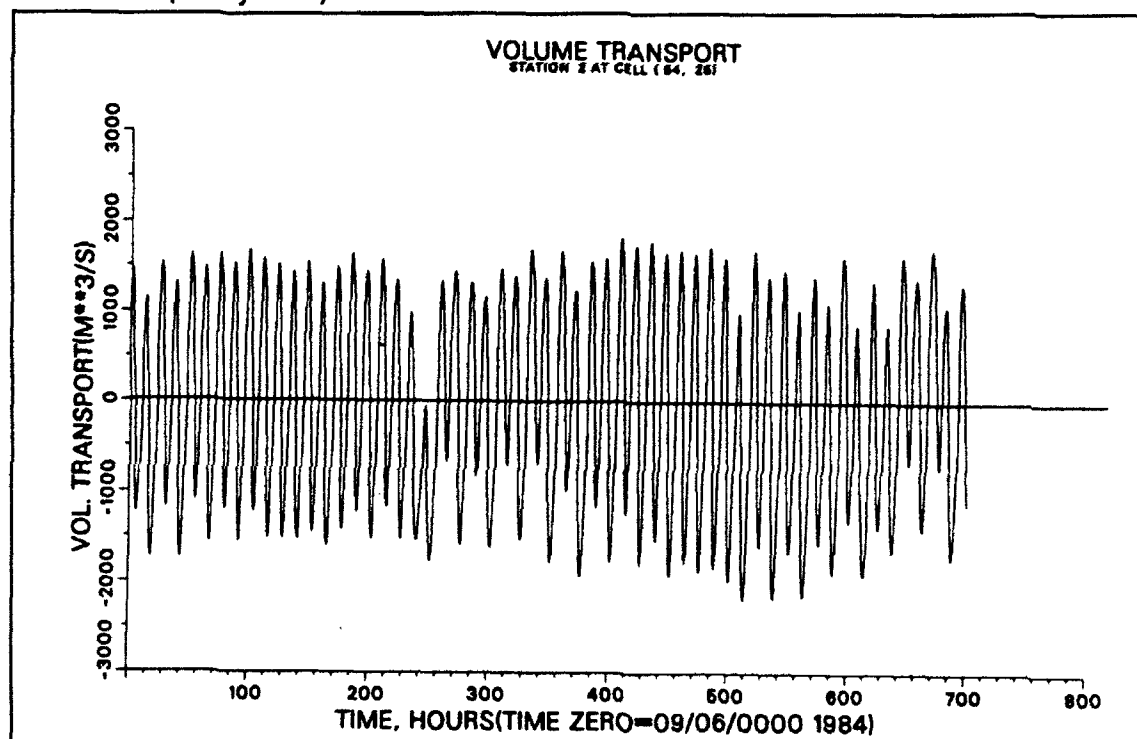


Figure 13b. Computed inter-tidal volume transport at Summit Bridge

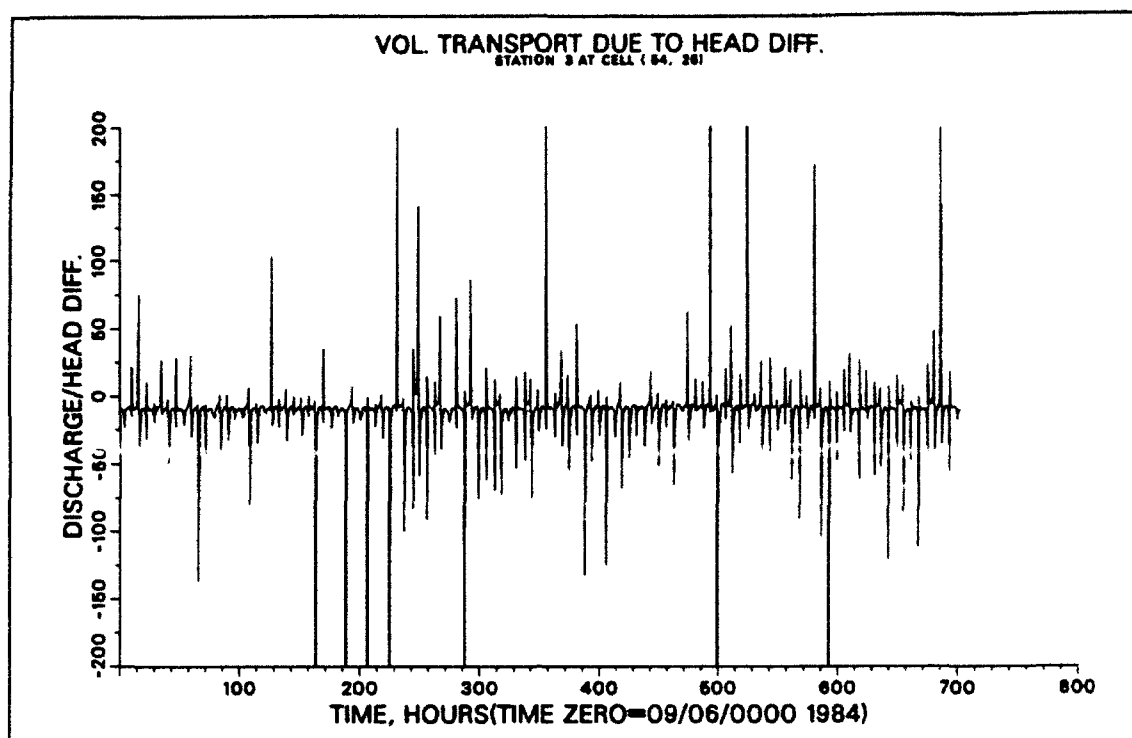


Figure 13c. Computed ratio of discharge to head difference with phase shift of  $\pm 1.5$  hours

ratios were obtained, the majority of the time the ratio was about -10. That indicates that the Reedy Point surface elevation was usually higher than that at Old Town Point and a nontidal flow of about  $10 \text{ m}^3/\text{s}$  was induced for every 1 cm head difference. This relationship can be more accurately identified by using the cross-spectral method.

To determine the accuracy of the model's ability to compute transport in the canal, Summit Bridge was chosen as a control station. The transport calculation was made by using half-hour values of surface elevation, tidal currents, and salinity concentrations from 57 tidal cycles. The tidal cycle durations ranged from 11.5 hours to 13.5 hours. Figures 14a-14d show tidal-average volume transport, cumulative average volume transport, and the corresponding net salt transport for the base run (40-foot channel in most of Upper Chesapeake Bay and the entire C&D canal). The maximum tidal-average volume transport was found from tidal cycle 22 to tidal cycle 23 due to a strong current variation for that period. The cumulative-average volume transport indicates that the computation of net transport requires a longer time period to reach equilibrium. These results show a westerly net volume transport of  $61.53 \text{ m}^3/\text{s}$  and a net salt transport of  $578.8 \text{ g/s}$  through the canal for this 57-tidal-cycles period.

The net transport using the September 1984 field measurements was computed by using the actual cross-section profile (Boicourt, 1987) and values of



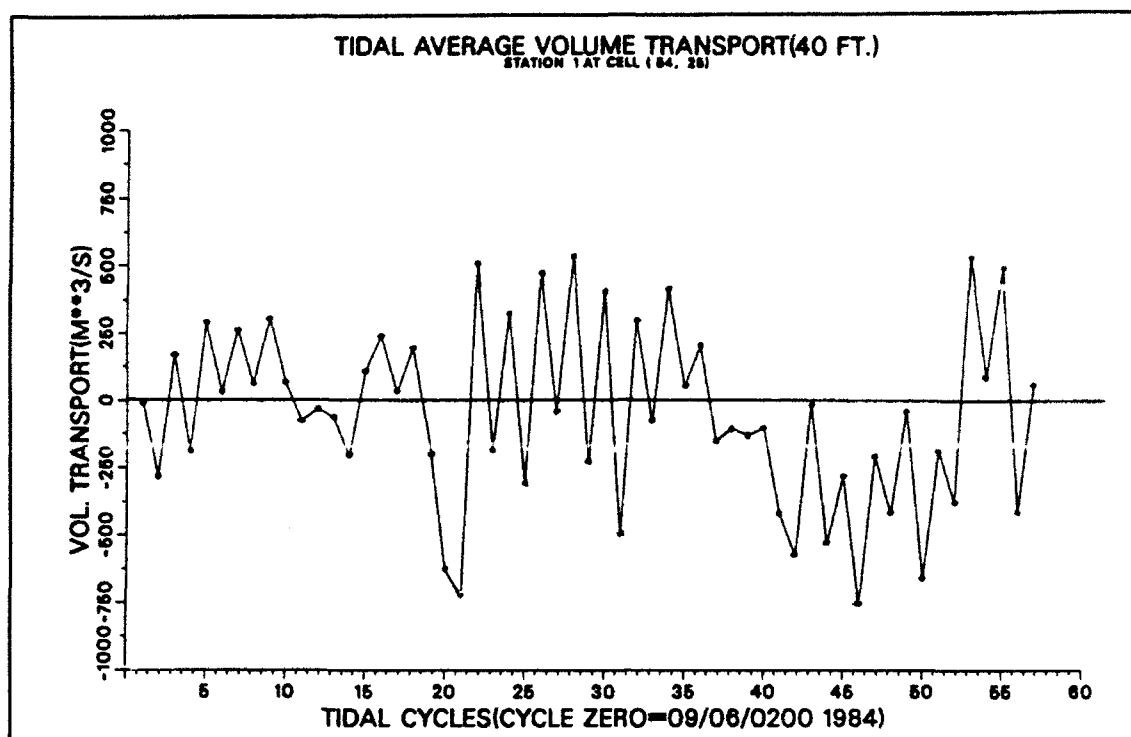


Figure 14a. Tidal average volume transport at Summit Bridge

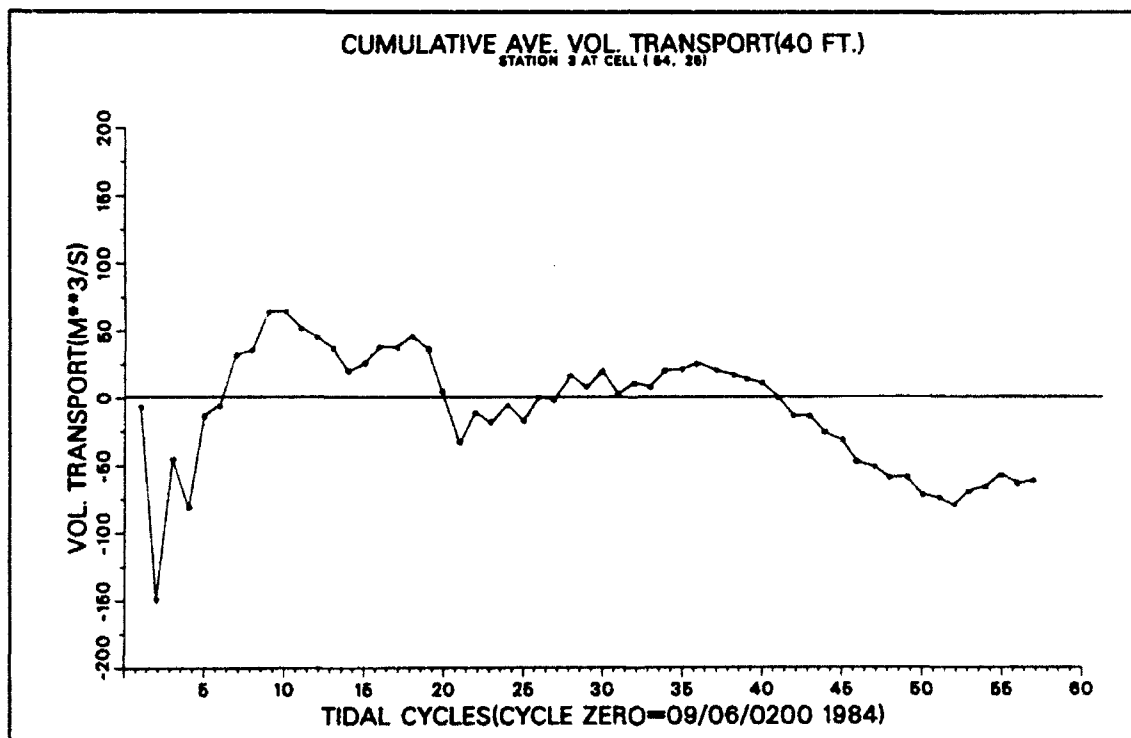


Figure 14b. Cumulative average volume transport at Summit Bridge

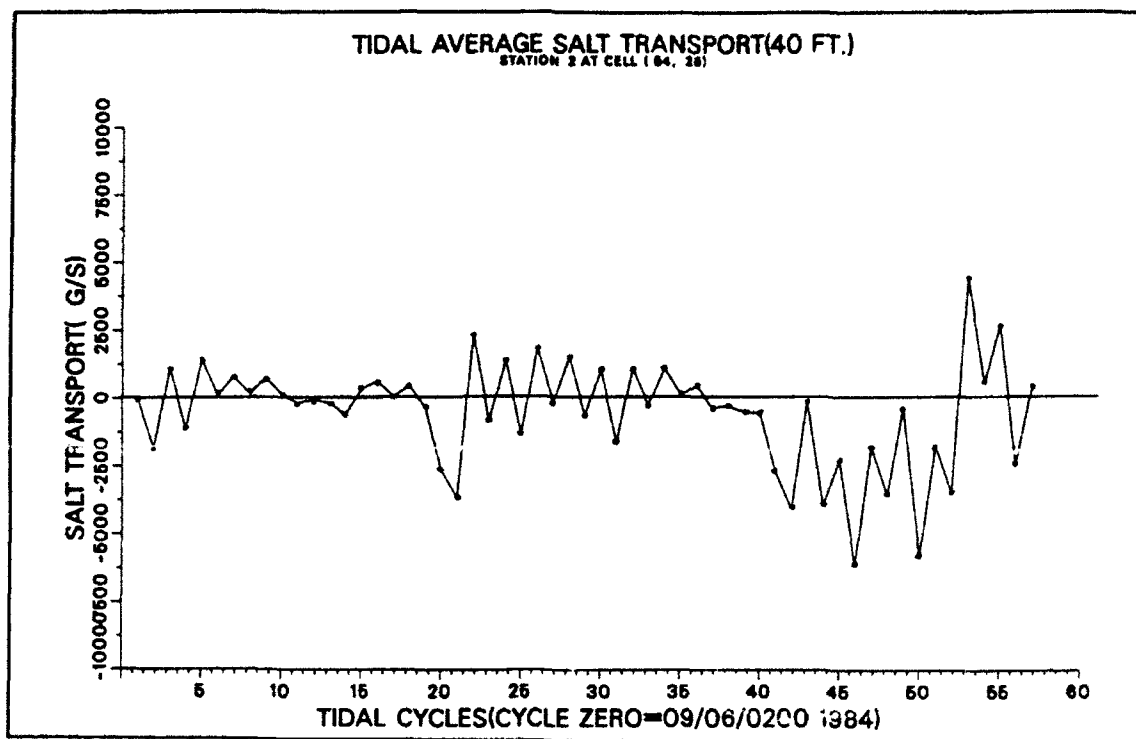


Figure 14c. Tidal average salt transport at Summit Bridge

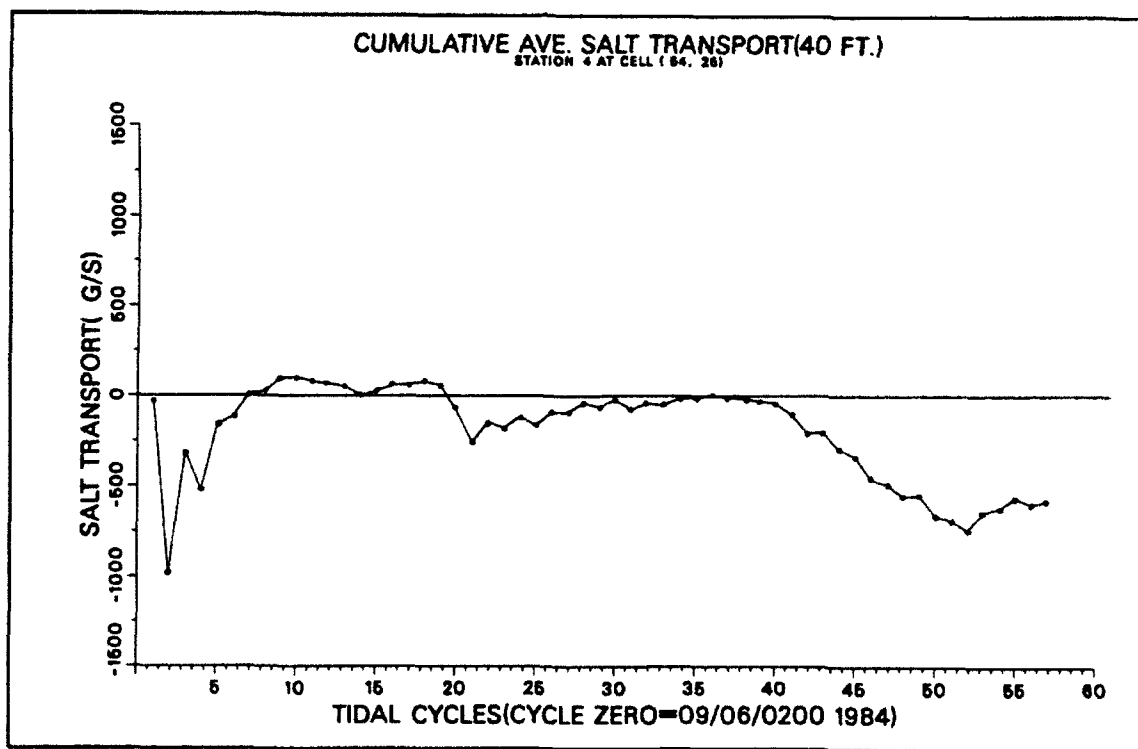


Figure 14d. Cumulative average salt transport at Summit Bridge

velocity and salinity from three current meters (Rives and Pritchard, 1978). The net volume and salt transport computed from the field data were  $57.1 \text{ m}^3/\text{s}$  and  $540.2 \text{ g/s}$  from the Delaware Bay to the Chesapeake Bay. The less than ten percent difference between model and prototype salt transport provides confidence in the use of the model.

The verified model was then run for two plans; namely, a 35 feet channel and a 45 feet channel. The 35 feet channel reduced the westerly flow (salt) transport about 16(17) percent. However, less variation was obtained by increasing the channel depth to 45 feet. These results are summarized in Table 3.

**Table 3**  
**Net Transport of Flow and Salt at Summit Bridge, C&D Canal for Month Long Simulation (57 Tidal Cycles)**

	Flow Transport $\text{m}^3/\text{s}$ ( $\text{ft}^3/\text{s}$ )	Normalized to base	Salt Transport $\text{gm/s}$	Normalized to base
35' plan (Model)	-51.6 <sup>1</sup> (-1785)	0.84	-478	0.83
40' Field	-57.1 (-1885)	0.93	-540	0.94
40' Base (Model)	-61.5 (-2160)	1.00	-578	1.00
45' plan (Model)	-70.1 (-2453)	1.14	-673	1.17

<sup>1</sup> Negative sign indicates westerly transport through the canal.

## 5 Conclusions and Recommendations

---

### Conclusions

A 3-D hydrodynamic model of the C&D canal and adjacent estuaries has been developed using CH3D-WES. The finite-difference numerical method was used to solve the governing equations of motion on a boundary-fitted grid, which allows for more accurate resolution of complex horizontal geometry than traditional rectilinear finite-difference grids. A special feature of the model is the use of a simplified vertical turbulence model based upon the assumption of local equilibrium of turbulence.

Using September 1984 as the test period, both model results and field data show a net transport in the C&D Canal in the westward direction. However, to determine the long-term net transport much longer simulations are required. Model results show that as the navigation channel is increased from 35 to 45 feet deep, the net flow transport increases about 30 percent with the salt transport increasing about 34 percent.

This model application demonstrates that a narrow channel, such as the C&D canal, connecting two dynamic water bodies can be successfully modelled using time-varying forcing functions with highly variable tides and salinities. The tidal elevations, tidal currents, and salinity were well-verified during a month-long simulation. The verification accuracy primarily depended on providing accurate tidal datums and salinity values at open boundaries.

The model has several potential uses other than studying channel deepening. Environmental impacts, such as larvae transport in Upper Chesapeake Bay, (particularly in the Elk River and Susquehanna Flats) can be addressed by using particle tracking methods which use the computational flow field from the model output. Secondly, the model can be used to evaluate river regulation, such as reservoir releases due to weather pattern changes, and to investigate water supply and saltwater intrusion problems. The model also can be used to conduct long term simulation tests with hypothetical boundary variation after verification to longer periods of time, e.g. seasons.

## Recommendations

Development of 3-D hydrodynamic models requires large field databases for model verification. Good current and salinity data are essential. Since such a data base does not exist for the modeled area, the following recommendations are offered in the design of a field data collection effort. To conduct a long-term simulation for verification, e.g. one year, the salinity boundary profiles at both Cape May-Lewes and Annapolis must be provided. Meters, collecting currents, salinity and temperature data at half-hour intervals will be sufficient. It is recommended that six of the meters be placed in two vertical strings at near-surface, mid-depth, and near-bottom for each string. The two strings should be located on both sides of the navigation channel to ensure redundancy. The tidal elevations can be obtained from NOAA, however, year long gauges probably should be installed since it is usually better if all data come from the same source to avoid methodology discrepancies. In addition, the NGVD information must be updated. For generating the initial salinity field and for verification purposes, interior monitoring stations must be established. Two stations in the Upper Chesapeake, three stations in the canal, and four stations in the Delaware (three in the lower Bay and one in the upper Bay) should be adequate.

# References

---

- Boyd, M. B., Bobb, W. H., Huval, C. J., and Hill, T. C., "Enlargement of the Chesapeake and Delaware Bay Canal-Hydraulic and Mathematical Model Investigation," Technical Report H-73-16, U.S. Army Waterways Experiment Station, Oct. 1973.
- Boicourt, W. "Flow and Salt Transport through the C&D Canal: Prediction from Wind Stress, Tidal Height, and Boundary Salinities," Dept. of Natural Resources, State of Maryland, Dec. 1987.
- Galperin, B. and Mellor G. L. "A Time-Dependent, Three-Dimensional Model of the Delaware Bay and River System Part I: Description of the Model and Tidal Analysis," *Estuarine, Coastal and Shelf Science* 31, 231-253. Nov. 1990.
- Galperin, B. and Mellor G. L. "A Time-Dependent, Three-Dimensional Model of the Delaware Bay and River System Part II: Three-Dimensional Flow Fields and Residual Circulation," *Estuarine, Coastal and Shelf Science* 31, 255-281. Nov. 1990.
- Gardner, G. B., and Pritchard, D. W., "Verification and Use of a Numerical Model of the Chesapeake and Delaware Bay Canal," Technical Report No. 87, CBI. The Johns Hopkins University, Baltimore, MD, July, 1974.
- Hires, R. I., Mellor, G. L., Oey, L.-Y. and Garvine, R. W. "Circulation of the Estuary In: The Delaware Estuary: Research and Background of Estuarine Management and Development (Sharp, J. H. ed)," Unpubl. report to the Delaware River and Bay Authority, Lewes, DE, pp. 27-49.
- Hsu, S. A. 1986. "Correction of Land-Based Wind Data for Offshore Applications: A Further Evaluation," *Journal of Physical Oceanography* 16 390-394, 1986.
- Johnson, B. H. "Mathematical Model Study of A Flow Control Plan for the Chesapeake and Delaware Canal" U.S. Army Engineer Waterways Experiment Station, Vicksburg, MS 39180.
- Johnson, B. H., Kim, K. W., Heath, R. E., Hsieh, B. B., and Butler, H. L. "Verification of a Three-Dimensional Numerical Hydrodynamic, Salinity,

and Temperature Model of Chesapeake Bay," Technical Report HL-91-7, U.S. Army Engineer Waterways Experiment Station, Vicksburg, MS. 1991.

Johnson, B. H., Heath, R. E. and Kim, K. W. "Development of A Three-Dimensional Hydrodynamic Model of Upper Chesapeake Bay," U.S. Army Engineer Waterways Experiment Station, Vicksburg, MS. Sep. 1989.

Kim, K. W. Johnson, B. H. and Sheng, Y. P. "Modeling A Wind-Mixing and Fall Turnover Event on Chesapeake Bay", Estuarine and Coastal Modeling Malcolm L. Spaulding (editor), Newport, Rhode Island Nov 1989 p 173-181.

Najarian, T. O., Thatcher, M. L. and Harleman, D. R. "C&D Canal Effect on Salinity of Delaware Estuary," Journal of the Waterway, Port, Coastal and Ocean Division, ASCE. Vol 106, No WW1, Feb. 1980.

Pritchard, D. W., and Gardner, G. B. "Hydrography of the C&D Canal," Technical Report No. 85, CBI, The Johns Hopkins University, Baltimore, MD, Feb., 1974.

Rives, S. R., and Pritchard, D. W. "Adaptation of J. R. Hunter's One-Dimensional Model to the C&D Canal System," Special Report No. 66, CBI, The Johns Hopkins University, Baltimore, MD. Oct., 1978.

Sheng, Y. P. "Hydraulic Applications of a Second-Order Closure Model of Turbulent Transport," Applying Research to Hydraulic Practice, CP. Smith, Ed.), ASCE, pp. 106-119, 1982.

Sheng, Y. P. "A Three-Dimensional Mathematical Model of Coastal, Estuarine and Lake Currents Using Boundary Fitted Grid," A.R.A.P. Group of Titan Systems New Jersey, Report No. 585, Princeton, NJ. 1986.

Thompson, J. F. and Johnson, B. H. "Development of an Adaptive Boundary-Fitted Coordinate Code for Use in Coastal and Estuarine Areas," MP-HL-85-5, US Army Engineer Waterways Experiment Station, Vicksburg, MS. 1985.

Wicker, C. F., "Tides and Currents in the Chesapeake and Delaware Bay Canal," Internal Memo, U.S. Army Corps of Engineers, Philadelphia District, Philadelphia, PA, Jan 1939.

REPORT DOCUMENTATION PAGE			Form Approved OMB No. 0704-0188	
<small>Public reporting burden for this collection of information is estimated to average 1 hour per response, including the time for reviewing instructions, searching existing data sources, gathering and maintaining the data needed, and completing and reviewing the collection of information. Send comments regarding this burden estimate or any other aspect of this collection of information, including suggestions for reducing this burden, to Washington Headquarters Services, Directorate for Information Operations and Reports, 1215 Jefferson Davis Highway, Suite 1204, Arlington, VA 22202-4302, and to the Office of Management and Budget, Paperwork Reduction Project (0704-0188), Washington, DC 20503.</small>				
1. AGENCY USE ONLY (Leave blank)	2. REPORT DATE May 1993	3. REPORT TYPE AND DATES COVERED Final report		
4. TITLE AND SUBTITLE A Three-Dimensional Numerical Model Study for the Chesapeake and Delaware Canal and Adjacent Bays		5. FUNDING NUMBERS		
6. AUTHOR(S) Bernard B. Hsieh Billy H. Johnson David R. Richards		8. PERFORMING ORGANIZATION REPORT NUMBER Technical Report HL-93-4		
7. PERFORMING ORGANIZATION NAME(S) AND ADDRESS(ES) U.S. Army Engineer Waterways Experiment Station Hydraulics Laboratory 3909 Halls Ferry Road, Vicksburg, MS 39180-6199		10. SPONSORING / MONITORING AGENCY REPORT NUMBER		
9. SPONSORING / MONITORING AGENCY NAME(S) AND ADDRESS(ES) U.S. Army Engineer District, Philadelphia 2nd and Chestnut Streets Philadelphia, PA 19106-2991		11. SUPPLEMENTARY NOTES Available from National Technical Information Service, 5285 Port Royal Road, Springfield, VA 22161.		
12a. DISTRIBUTION / AVAILABILITY STATEMENT  Approved for public release; distribution is unlimited.		12b. DISTRIBUTION CODE		
13. ABSTRACT (Maximum 200 words) <p>Flow problems in the Chesapeake and Delaware (C&amp;D) Canal, Maryland and Delaware, have received much attention over the years. However, due to the complex interactions of forcing functions and the sensitivity of flow conditions in the canal to hydraulic head differences, previous investigators have been unable to completely resolve many questions. To better understand the effect of one estuarine system on the other and to accurately compute flow and mass fluxes through the canal, a three-dimensional numerical hydrodynamic model extending from the Chesapeake Bay Bridge at Annapolis, MD, through the C&amp;D Canal and connecting with a grid extending from Trenton, NJ, to the mouth of Delaware Bay was developed.</p> <p>The model was initially tested by analyzing the propagation of tidal waves without considering salinity. An inset model that consisted of only the C&amp;D canal was used to examine the sensitivity of results to wind stress, nonlinear terms in the equations of motion, an entrance loss term at both ends of the canal, bottom drag coefficients, and the effect of tidal datums. The information gained from the inset grid tests was then extended to the full hydrodynamic-salinity model. The tidal elevations, tidal currents, and salinity were well-verified during a</p> <p style="text-align: right;">(Continued)</p>				
14. SUBJECT TERMS Chesapeake Mathematical Delaware Numerical Hydrodynamics Three-Dimensional		15. NUMBER OF PAGES 55		
		16. PRICE CODE		
17. SECURITY CLASSIFICATION OF REPORT UNCLASSIFIED	18. SECURITY CLASSIFICATION OF THIS PAGE UNCLASSIFIED	19. SECURITY CLASSIFICATION OF ABSTRACT	20. LIMITATION OF ABSTRACT	



13. (Concluded).

month-long simulation using September, 1984 data. Verification accuracy depended primarily on providing correct tidal and salinity values at open boundaries.

The verified model was then used to compute net transport through the C&D Canal for a range of channel depths. Computed results showed a westerly net transport of  $61.53 \text{ m}^3/\text{sec}$  and a net salt transport of  $0.58 \text{ g/sec}$  through the canal for a 40-ft depth over the one month-long simulation. The model has other potential uses, e.g., to address larvae transport in the Upper Chesapeake Bay, to evaluate river regulation, to investigate water supply and saltwater intrusion, and to compute long-term simulations with hypothetical boundary variations representing possible regional management alternatives.